The Meteoritical Society

Meteoritics & Planetary Science 42, Nr 4/5, 689–708 (2007)
Abstract available online at http://meteoritics.org

Drill core LB-08A, Bosumtwi impact structure, Ghana: Geochemistry of fallback breccia and basement samples from the central uplift

Ludovic FERRIÈRE[1*], Christian KOEBERL[1], Wolf Uwe REIMOLD[2], and Dieter MADER[1]

[1]Department of Geological Sciences, University of Vienna, Althanstrasse 14, A-1090 Vienna, Austria
[2]Museum of Natural History (Mineralogy), Humboldt University, Invalidenstrasse 43, D-10115 Berlin, Germany
[*]Corresponding author. E-mail: ludovic.ferriere@univie.ac.at

(Received 16 September 2006; revision accepted 01 January 2007)

Abstract–The 1.07 Myr old Bosumtwi impact structure in Ghana (West Africa), which measures 10.5 km in diameter and is largely filled by Lake Bosumtwi, is associated with one of four currently known tektite strewn fields. Two boreholes were drilled to acquire hard-rock samples of the deep crater moat and from the flank of the central uplift (LB-07A and LB-08A, respectively) during a recent ICDP-sponsored drilling project.

Here we present results of major and trace element analysis of 112 samples from drill core LB-08A. This core, which was recovered between 235.6 and 451.33 m depth below lake level, contains polymict lithic breccia intercalated with suevite, which overlies fractured/brecciated metasediment. The basement is dominated by meta-graywacke (from fine-grained to gritty), but also includes some phyllite and slate, as well as suevite dikelets and a few units of a distinct light greenish gray, medium-grained meta-graywacke.

Most of the variations of the major and trace element abundances in the different lithologies result from the initial compositional variations of the various target rock types, as well as from aqueous alteration processes, which have undeniably affected the different rocks.

Suevite from core LB-08A (fallback suevite) and fallout suevite samples (from outside the northern crater rim) display some differences in major (mainly in MgO, CaO, and Na_2O contents) and minor (mainly Cr and Ni) element abundances that could be related to the higher degree of alteration of fallback suevites, but also result from differences in the clast populations of the two suevite populations. For example, granite clasts are present in fallout suevite but not in fallback breccia, and calcite clasts are present in fallback breccia and not in fallout suevite. Chondrite-normalized rare earth element abundance patterns for polymict impact breccia and basement samples are very similar to each other.

Siderophile element contents in the impact breccias are not significantly different from those of the metasediments, or compared to target rocks from outside the crater rim. So far, no evidence for a meteoritic component has been detected in polymict impact breccias during this study, in agreement with previous work.

INTRODUCTION

The 1.07 Myr old, well-preserved Bosumtwi impact structure (centered at 06°30′N, 01°25′W) is situated in the Ashanti region of Ghana, West Africa. It is a complex impact structure, 10.5 km in diameter, with a pronounced rim and a small central uplift (Scholz et al. 2002). The crater is mostly filled by Lake Bosumtwi, which is ~8 km in diameter. The Bosumtwi impact structure is also associated with the Ivory Coast tektites, on the basis of the geographical location of the tektite strewn field, as well as identical ages and matching chemical and isotopic compositions of the tektites and the Bosumtwi crater rocks (Schnetzler et al. 1966, 1967; Gentner et al. 1967, 1969; Kolbe et al. 1967; Jones 1985; Koeberl et al. 1997). Bosumtwi was recently the subject of an international and multidisciplinary drilling project by the International Continental Scientific Drilling Program (ICDP; see below and Koeberl et al. 2007 for more information).

Here, we present results of major and trace element analysis of 112 samples from drill core LB-08A. We also provide a brief comparison of chemical data for LB-08A (fallback breccia and basement) samples with those for

Bosumtwi target rocks and suevite from the fallout deposit sampled to the north of the crater structure.

GEOLOGICAL SETTING AND SAMPLES

Geological Setting and Previous Work

Geological investigations around Lake Bosumtwi were first performed in the 1930s (Junner 1937) and continued in the 1960s (Woodfield 1966; Moon and Mason 1967; Jones et al. 1981). A new geological map (Koeberl and Reimold 2005) summarizes the results of these early studies but also includes observations on new outcrops revealed by recent road construction as well as observations obtained from shallow drilling on and beyond the northern crater rim (Boamah and Koeberl 2003). The crater was formed in lower greenschist facies metasediments of the 2.1–2.2 Gyr Birimian Supergroup (Wright et al. 1985; Leube et al. 1990). The Birimian Supergroup rocks consist of an assemblage of metasediments, including phyllites, meta-tuffs, meta-graywackes, quartzitic meta-graywackes, shales, and slates (Koeberl and Reimold 2005). Proterozoic granitic intrusions, weathered granitoid dikes, and dolerite and amphibolite dikes are also present in the region around the crater (e.g., Junner 1937; Woodfield 1966; Moon and Mason 1967; Reimold et al. 1998). Numerous outcrops of breccia were identified in the environs of the crater (e.g., Junner 1937; Woodfield 1966; Moon and Mason 1967), but it is not clear whether or not all breccias are impact-related (Reimold et al. 1998). On the basis of composition and texture, Boamah and Koeberl (2003) distinguished three types of impact breccia at the Bosumtwi crater: an autochthonous monomict breccia (occurs on the northern part of the crater rim), a probably allochthonous polymict lithic impact breccia (also to the north of the crater rim), and a suevitic breccia (occurs to the north and south of the crater and along the northern crater rim; contains impact melt fragments and a variety of country rock clasts [meta-graywacke, phyllite, shale, and granite] of up to about 40 cm in size).

Target rocks from outside the crater rim and suevite samples from the crater rim were analyzed earlier for their major and trace element compositions (Koeberl et al. 1998; Boamah and Koeberl 2003; Dai et al. 2005; soils from the environs of the Bosumtwi crater were also analyzed for their elemental abundances by Boamah and Koeberl [2002]), and some samples were analyzed for their O, Sr, and Nd isotopic compositions (Koeberl et al. 1998).

Drill Core LB-08A

The core LB-08A was drilled on the outer flank of the central uplift, into the crater fill and underlying basement, to a depth of 451.33 m. Located in the northwestern part of the uplift structure (6°30′33″N, 1°24′45″E), the drilling was situated on seismic survey lines that were established during the preparation phase of the drilling project (see Koeberl et al. 2007 for more information). The central uplift was identified on multichannel seismic reflection profiles; it has an apparent diameter of 1.9 km and a maximum height of about 130 m above the surrounding moat (e.g., Scholz et al. 2002).

The drill core displays a variety of lithologies (in order of decreasing abundance): meta-graywacke, slate, phyllite, polymict impact breccia, and monomict lithic impact breccia. The distinction and characterization of the different rock types is based on petrographic observations, and the classification follows definitions by Stöffler and Grieve (1994) for impact breccia, and Jackson (1997) and Brodie et al. (2004) for metasediments (more details are provided in Ferrière et al. 2007). The core can be divided into two main parts: the uppermost 25 m that are composed of polymict lithic impact breccia (clast-supported) intercalated with suevite (containing melt fragments), and the other part of the core (between 262 to 451 m) which is dominated by autochthonous, fractured/brecciated metasediment, which is locally brecciated (monomict lithic breccia) and intersected by suevite dikelets.

The upper part of the core, between 235.6 and 262 m (Fig. 1), has been interpreted as a fallback impact breccia deposit (Ferrière et al. 2007). This suevite has a fine-grained fragmental matrix (39 to 45 vol%) and contains a variety of lithic clasts and mineral fragments: meta-graywacke, phyllite, slate, quartzite, carbon-rich organic shale, and calcite, as well as impact-melt particles, diaplectic quartz glass, unshocked quartz, fractured quartz, quartz with shock-characteristic planar deformation features (PDFs; up to 4 sets of different orientations), phyllosilicate minerals, epidote, sphene, and opaque minerals.

The lower part of the core (Fig. 2), between 262 and 451 m, represents the crater basement, which has been shocked (as shown by, e.g., the presence of PDFs in quartz grains) and fractured in situ during the formation of the impact crater (for more information on drill core LB-08A, see Ferrière et al. 2007). The sharp transition from impact breccia to basement is located at a depth of ~262 m below lake level. The basement is composed of an alternating sequence of metasediment comprising (in order of decreasing abundance) meta-graywacke (dominant), phyllite, and slate, with locally occurring monomict lithic breccia, light greenish gray, medium-grained meta-graywacke (which contains some clasts of granophyric material), and suevite dikelets (likely injections into the metasediment, up to 80 cm thick; occurring between 279.5 and 298 m and between 418 and 440 m). The metasediment displays a large variation in lithology and grain size (from fine-grained to gritty; Ferrière et al. 2007).

Samples from the central uplift display a variety of alteration effects: alteration of plagioclase to sericite, biotite

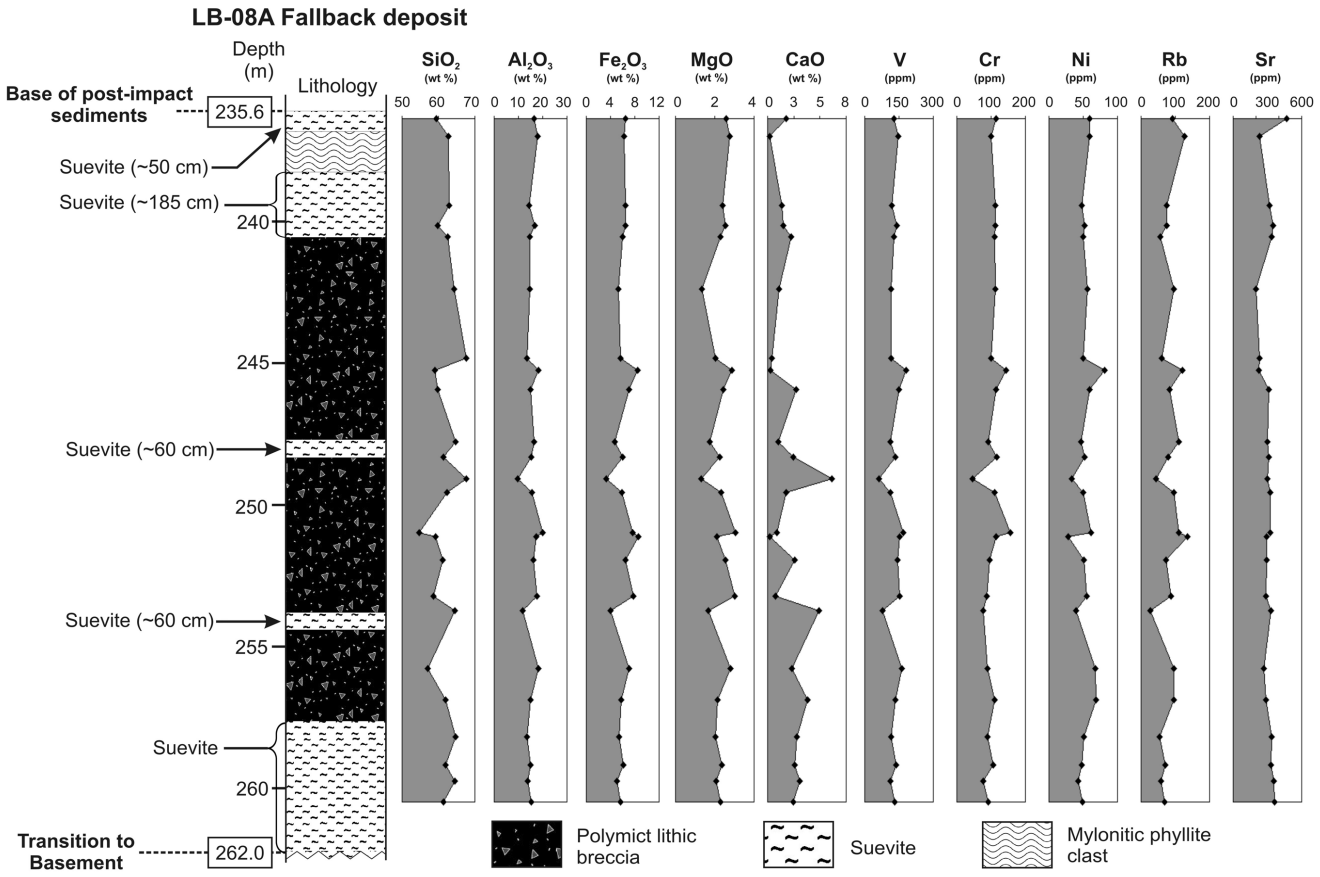

Fig. 1. Lithostratigraphy of the uppermost part (fallback deposit; between 235.6 to 262 m) of core LB-08A into the central uplift of the Bosumtwi impact structure, comparing the variations of concentrations of some major (SiO_2, Al_2O_3, Fe_2O_3, MgO, and CaO) and trace (V, Cr, Ni, Rb, and Sr) elements with depth.

to chlorite, fractures that are filled with iron oxides, secondary pyrite, and secondary calcite veinlets and aggregates, and the matrices of polymict impact breccias are composed to a large degree of very fine-grained phyllosilicates (Ferrière et al. 2007). Calcite veinlets and aggregates in suevite samples from the fallback deposit have been interpreted as the result of hydrothermal circulation in the rock after the impact event (Ferrière et al. 2007). No systematic change regarding the intensity of secondary alteration throughout the core has been identified in that detailed petrographic study.

Samples

One hundred and twenty one samples, comprising all lithologies present, were taken from core LB-08A, between 235.77 m (KR8-001) and 451.23 m (KR8-125) depth, in order to cover the complete variety of different lithologies present in the core (Ferrière et al. 2007). One hundred and twelve samples, comprising polymict lithic impact breccia (13 samples), suevite (20 samples), meta-graywacke (67 samples), slate-phyllite (8 samples), and light greenish gray meta-graywacke (4 samples) were analyzed.

EXPERIMENTAL METHODS

Samples with masses ranging from 30 to 500 g were taken from drill core LB-08A during the sampling party at the GeoForschungsZentrum (GFZ) in Potsdam, Germany, where the core is kept at ICDP headquarters. Samples were cut at the GFZ and mailed to Vienna. Representative aliquots weighing about 20 to 30 g of these samples were crushed in polyethylene wrappers and powdered in a mechanical agate mill for bulk chemical analysis. Special attention was paid to avoid clasts larger than 5 mm in diameter for the impact breccia samples, to obtain relatively representative compositions. Due to the variable abundance of matrix (from less than 2 to 48 vol%) in the polymict lithic impact breccia samples (Ferrière et al. 2007), and also due to the occurrence of some clasts larger than the core diameter, some minor heterogeneities can result from the restrictions of the sample preparation.

The contents of major and trace elements (V, Cr, Co, Ni, Cu, Zn, Rb, Sr, Y, Zr, Nb, and Ba) were determined by standard X-ray fluorescence (XRF) spectrometry at the University of the Witwatersrand, Johannesburg (South

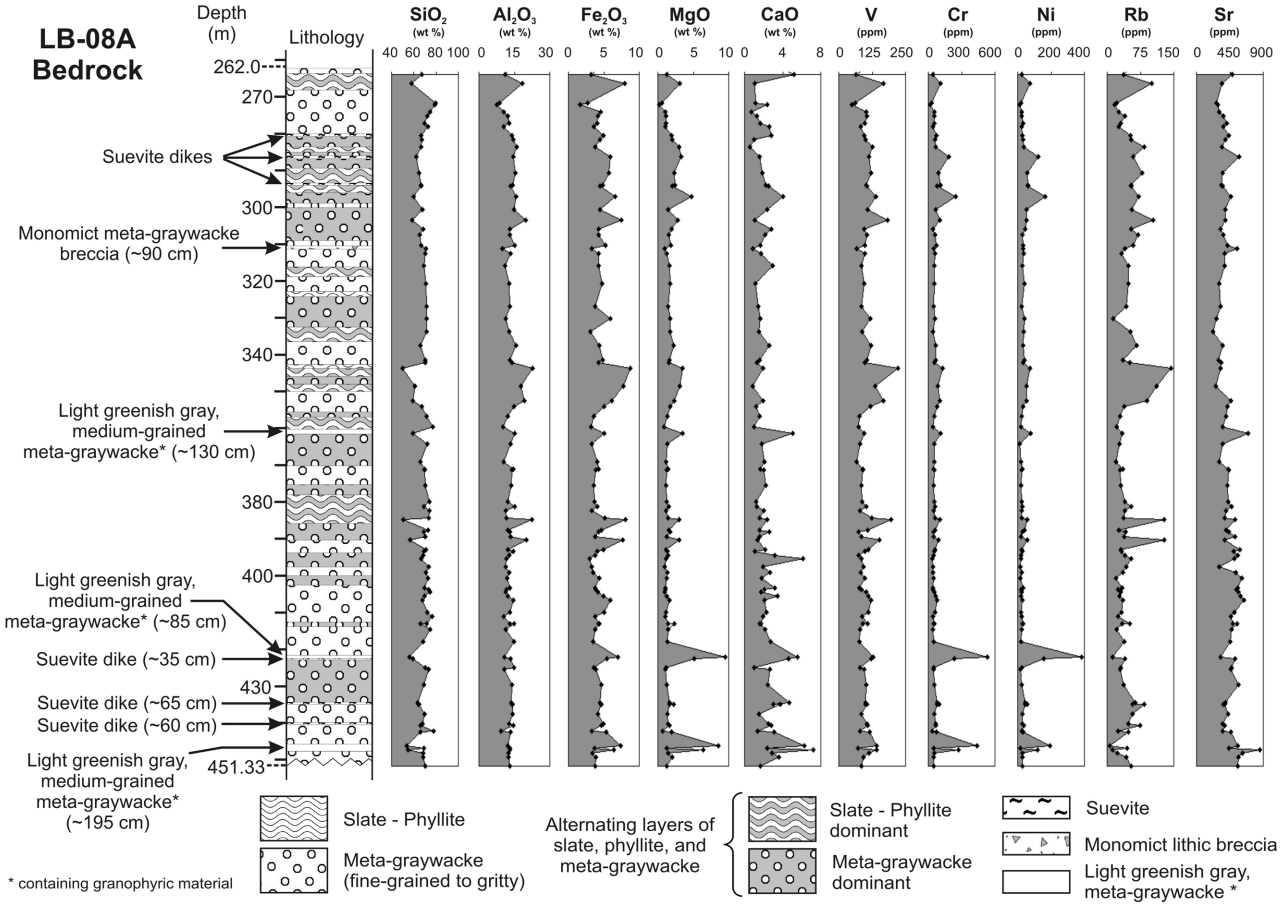

Fig. 2. Lithostratigraphy of the basement section (between 262 to 451.33 m) of core LB-08A into the central uplift of the Bosumtwi impact structure, comparing the variation of concentrations of some major (SiO_2, Al_2O_3, Fe_2O_3, MgO, and CaO) and trace (V, Cr, Ni, Rb, and Sr) elements with depth.

Africa). Precision and accuracy values are (in wt%) about 0.4 for SiO_2, 0.03 for TiO_2, 0.2 for Al_2O_3 and MgO, 0.1 for Fe_2O_3, CaO and K_2O, 0.01 for MnO and P_2O_5, and 0.3 for Na_2O (for more details, see Reimold et al. 1994).

Abundances of some major elements (Fe, Na, and K) and other trace elements (Sc, Cr, Co, Ni, Zn, As, Se, Br, Rb, Sr, Zr, Sb, Cs, Ba, Hf, Ta, Th, and U), including the rare earth elements (REE), were determined by instrumental neutron activation analysis (INAA) at the Department of Geological Sciences, University of Vienna (Austria). About 160 mg of each sample powder and about 90 mg of several international rock standards: the carbonaceous chondrite Allende (Smithsonian Institution, Washington, USA; Jarosewich et al. 1987), granite ACE (Centre de Recherche Pétrographique et Géochimique, Nancy, France; Govindaraju 1994), and granite G-2 (USGS; Govindaraju 1994) were sealed in polyethylene capsules. Samples and standards were irradiated together in the 250 kW Triga reactor of the Atomic Institute of the Austrian Universities for 8 hours at a neutron flux of 2.10^{12} n · cm^{-2} · s^{-1}. More details on instrumentation, as well as accuracy and precision values of our method, have been described in, e.g., Koeberl (1993) and Son and Koeberl (2005). For all samples, the Fe, Na, K, Cr, Co, Ni, Zn, Rb, Sr, Zr, and Ba concentrations were determined by both XRF and INAA.

RESULTS

The major and trace element contents of the 112 LB-08A samples are summarized in the form of average compositions for each different lithology (Table 1). Individual data are not listed here, but will be published elsewhere. To allow discussion of the general geochemical patterns of the samples investigated in this study, the contents of some major (SiO_2, Al_2O_3, Fe_2O_3, MgO, and CaO) and trace (V, Cr, Ni, Rb, and Sr) elements have been plotted against depth in the uppermost part (fallback deposit) and the basement section of core LB-08A, and are shown in Figs. 1 and 2, respectively. These specific trace elements have been selected because of the extent of their relative abundance variations between the various lithologies and also within each lithological type. Elements the abundances of which show significant

Table 1. The average and range of compositions of analyzed samples from borehole LB-08A, compared to those of fallout suevites, target rocks, and Ivory Coast tektites.[a]

	Suevite (n = 20)		Polymict lithic impact breccia (n = 13)		Meta-graywacke (n = 67)		Phyllite-slate (n = 8)	
	Average	Range	Average	Range	Average	Range	Average	Range
SiO_2	63.16 ± 2.44	59.01–66.79	61.44 ± 3.92	54.80–67.74	70.68 ± 3.18	65.49–79.73	57.85 ± 5.19	50.14–64.41
TiO_2	0.55 ± 0.09	0.43–0.70	0.63 ± 0.15	0.28–0.81	0.41 ± 0.07	0.15–0.57	0.69 ± 0.15	0.40–0.95
Al_2O_3	14.65 ± 1.01	13.33–16.68	15.70 ± 2.84	9.64–20.12	12.67 ± 1.72	7.47–15.99	19.20 ± 2.68	14.59–22.86
Fe_2O_3	5.49 ± 0.74	4.44–6.63	6.34 ± 1.65	3.31–8.64	4.07 ± 0.73	1.64–5.93	7.39 ± 1.11	5.25–8.71
MnO	0.06 ± 0.01	0.05–0.09	0.07 ± 0.02	0.03–0.10	0.05 ± 0.02	0.03–0.17	0.06 ± 0.02	0.04–0.10
MgO	2.50 ± 0.93	1.62–5.16	2.31 ± 0.54	1.30–3.04	1.39 ± 0.41	0.24–2.99	2.82 ± 0.63	1.33–3.45
CaO	2.67 ± 0.98	1.38–4.72	2.19 ± 1.88	0.20–6.14	2.05 ± 0.94	0.60–6.14	1.26 ± 0.65	0.23–2.35
Na_2O	2.94 ± 0.36	2.05–3.58	2.73 ± 0.62	1.85–4.00	3.77 ± 0.71	2.30–5.61	2.37 ± 0.60	1.75–3.30
K_2O	1.67 ± 0.36	0.87–2.37	2.08 ± 0.69	0.77–2.93	0.99 ± 0.39	0.29–2.25	2.94 ± 0.94	1.08–4.03
P_2O_5	0.11 ± 0.02	0.08–0.15	0.12 ± 0.04	0.04–0.21	0.09 ± 0.02	0.03–0.15	0.18 ± 0.13	0.08–0.44
LOI	5.25 ± 0.87	3.67–7.01	5.25 ± 1.03	3.15–6.81	3.10 ± 1.61	1.53–9.44	4.90 ± 2.10	3.76–9.99
Total	99.06		98.86		99.26		99.66	
Sc	14.0 ± 2.6	9.7–18.2	17.9 ± 5.3	7.2–25.4	8.2 ± 1.8	3.1–13.2	20.5 ± 3.5	16.9–26.6
V	117 ± 14	96–142	135 ± 35	63–180	93 ± 16	50–127	166 ± 34	117–222
Cr	115 ± 51	71–249	103 ± 28	46–156	54 ± 11	21–79	105 ± 13	86–130
Co	17 ± 4	12–26	18 ± 6	8–27	10 ± 2	3–15	22 ± 4	17–27
Ni	65 ± 37	31–165	53 ± 15	28–82	27 ± 8	11–52	61 ± 9	53–76
Cu	27 ± 9	11–43	41 ± 21	8–90	24 ± 16	2–83	44 ± 12	28–64
Zn	66 ± 11	50–84	74 ± 19	43–103	43 ± 9	11–64	94 ± 12	82–111
As	14.3 ± 12.5	3.73–51.9	10.7 ± 8.0	1.35–24.9	4.09 ± 3.71	0.09–14.1	10.9 ± 11.8	0.91–29.3
Rb	67 ± 15	39–97	86 ± 31	28–135	38 ± 13	14–84	117 ± 17	97–143
Sr	387 ± 72	314–575	291 ± 32	226–329	434 ± 100	225–638	333 ± 103	203–522
Y	16 ± 4	12–23	21 ± 5	13–28	11 ± 2	7–17	20 ± 3	16–25
Zr	126 ± 15	103–152	134 ± 24	76–164	117 ± 21	56–171	122 ± 9	112–132
Nb	3.8 ± 0.7	3–5	4.7 ± 0.9	3–6	3.3 ± 0.4	3–4	5.5 ± 0.8	5–7
Sb	0.40 ± 0.16	0.22–0.69	0.36 ± 0.23	0.08–1.01	0.36 ± 0.24	0.03–0.98	0.38 ± 0.14	0.20–0.57
Cs	4.30 ± 1.42	2.50–7.31	4.34 ± 1.63	1.66–7.29	2.29 ± 0.85	1.00–5.74	5.76 ± 1.19	3.74–7.58
Ba	626 ± 124	322–803	742 ± 267	258–1129	537 ± 163	244–972	1023 ± 232	612–1279
La	20.5 ± 3.3	15.1–27.0	18.5 ± 4.7	9.2–25.4	19.3 ± 4.52	11.6–33.0	20.0 ± 2.4	17.1–25.2
Ce	42.4 ± 6.7	32.0–59.2	38.9 ± 10.4	16.8–51.8	38.9 ± 7.91	23.7–64.2	43.7 ± 5.0	38.8–53.1
Nd	20.8 ± 4.0	14.2–30.3	19.4 ± 5.5	9.4–26.1	16.7 ± 3.15	11.7–25.9	20.9 ± 2.4	18.2–25.5
Sm	3.91 ± 0.78	2.57–5.63	3.97 ± 1.00	1.74–5.67	2.95 ± 0.49	1.86–4.25	4.25 ± 0.48	3.72–4.97
Eu	1.13 ± 0.19	0.74–1.52	1.07 ± 0.27	0.47–1.54	0.89 ± 0.13	0.55–1.20	1.22 ± 0.20	1.00–1.57
Gd	3.36 ± 0.45	2.74–4.09	3.27 ± 0.85	1.87–5.12	2.52 ± 0.61	1.04–4.08	4.14 ± 1.20	2.84–5.87
Tb	0.49 ± 0.11	0.27–0.70	0.54 ± 0.12	0.32–0.75	0.39 ± 0.11	0.19–0.65	0.61 ± 0.13	0.46–0.84
Tm	0.23 ± 0.05	0.15–0.34	0.31 ± 0.08	0.20–0.45	0.17 ± 0.03	0.11–0.23	0.28 ± 0.04	0.22–0.32
Yb	1.50 ± 0.31	1.10–2.11	2.09 ± 0.55	1.26–3.11	1.12 ± 0.17	0.64–1.63	1.83 ± 0.22	1.50–2.13
Lu	0.24 ± 0.04	0.18–0.31	0.33 ± 0.09	0.20–0.50	0.18 ± 0.03	0.10–0.27	0.29 ± 0.04	0.23–0.36
Hf	3.12 ± 0.35	2.49–3.65	3.35 ± 0.71	1.61–4.29	3.07 ± 0.71	1.20–5.09	3.00 ± 0.19	2.75–3.24

Table 1. *Continued.* The average and range of compositions of analyzed samples from borehole LB-08A, compared to those of fallout suevites, target rocks, and Ivory Coast tektites.[a]

	Suevite (n = 20)		Polymict lithic impact breccia (n = 13)		Meta-graywacke (n = 67)		Phyllite-slate (n = 8)	
	Average	Range	Average	Range	Average	Range	Average	Range
Ta	0.32 ± 0.05	0.23–0.42	0.36 ± 0.09	0.17–0.49	0.30 ± 0.08	0.13–0.58	0.56 ± 0.23	0.31–0.95
W	2.70 ± 1.51	0.08–6.17	3.30 ± 1.44	0.73–6.11	1.84 ± 1.59	0.05–5.45	3.00 ± 1.05	1.73–4.18
Th	3.17 ± 0.65	1.95–4.84	3.31 ± 0.61	2.28–3.95	2.91 ± 0.67	1.58–4.42	3.63 ± 0.33	3.27–4.18
U	1.39 ± 0.68	0.71–3.25	1.42 ± 0.83	0.61–3.02	1.07 ± 0.57	0.26–3.36	1.02 ± 0.34	0.65–1.50
K/U	12,018 ± 4946	3877–20,958	15,751 ± 8611	2117–30,685	9518 ± 5467	2245–28,896	27,716 ± 14,327	5996–49,525
Zr/Hf	40.4 ± 3.7	34.6–52.2	40.3 ± 2.9	36.2–47.1	38.7 ± 4.15	26.1–47.1	40.6 ± 2.3	35.6–43.1
La/Th	6.57 ± 0.84	5.25–8.40	5.71 ± 1.47	2.36–7.90	6.69 ± 0.85	3.80–9.01	5.52 ± 0.62	4.53–6.57
Hf/Ta	9.94 ± 0.92	8.01–11.3	9.50 ± 1.42	7.60–12.7	10.6 ± 2.23	6.05–16.4	6.13 ± 2.41	3.25–9.96
Th/U	2.77 ± 1.18	0.93–5.36	3.04 ± 1.52	0.76–5.42	3.25 ± 1.43	0.82–10.6	3.89 ± 1.19	2.64–5.40
La_N/Yb_N	9.51 ± 2.00	5.49–12.4	6.34 ± 2.12	2.64–10.5	11.8 ± 2.61	4.82–18.5	7.50 ± 1.47	6.33–10.4
Eu/Eu*	0.98 ± 0.05	0.91–1.09	0.91 ± 0.07	0.80–1.03	1.01 ± 0.11	0.81–1.51	0.88 ± 0.06	0.82–0.95
CIA	56	47–63	60	38–73	54	41–69	67	64–73

[a]Major element data in wt%, trace element data in ppm. All Fe as Fe_2O_3. n = number of samples; N = chondrite-normalized (Taylor and McLennan 1985); chemical index of alteration (CIA) = $(Al_2O_3/[Al_2O_3 + CaO + Na_2O + K_2O]) \times 100$ in molecular proportions. All ratios are the average of the ratios calculated for each samples.

Table 1. *Continued*. The average and range of compositions of analyzed samples from borehole LB-08A, compared to those of fallout suevites, target rocks, and Ivory Coast tektites.[a]

	Metasediments[b] (n = 75)		Light greenish gray meta-graywacke (n = 4)		Fallout suevite (n = 11)[c]	Meta-graywacke and phyllite (n = 7)[d]	Granite dike (n = 2)[d]	Pepiakese granite (n = 3)[d]	Ivory Coast tektites[d]
	Average	Range	Average	Range	Average	Average	Average	Average	Average
SiO_2	69.17 ± 5.34	50.14–79.73	55.91 ± 2.59	53.49–59.48	63.58 ± 3.01	66.75 ± 1.77	68.74 ± 0.50	57.81 ± 6.28	67.58
TiO_2	0.44 ± 0.12	0.15–0.95	0.65 ± 0.05	0.58–0.68	0.64 ± 0.07	0.66 ± 0.07	0.50 ± 0.00	0.46 ± 0.34	0.56
Al_2O_3	13.44 ± 2.79	7.47–22.86	12.81 ± 1.83	10.78–15.12	15.58 ± 1.15	15.27 ± 1.31	15.91 ± 0.18	16.45 ± 2.42	16.74
Fe_2O_3	4.44 ± 1.30	1.64–8.71	6.45 ± 1.01	5.05–7.34	6.58 ± 2.24	6.37 ± 0.62	3.97 ± 0.31	6.09 ± 3.97	6.16
MnO	0.05 ± 0.02	0.03–0.17	0.10 ± 0.01	0.08–0.11	0.11 ± 0.05	0.028 ± 0.009	0.014 ± 0.013	0.067 ± 0.047	0.06
MgO	1.56 ± 0.63	0.24–3.45	6.97 ± 2.66	3.48–9.48	1.43 ± 0.54	2.12 ± 0.25	1.44 ± 0.36	6.63 ± 4.61	3.46
CaO	1.96 ± 0.93	0.23–6.14	6.02 ± 0.93	5.06–7.19	1.39 ± 0.61	0.19 ± 0.13	0.31 ± 0.01	4.36 ± 2.94	1.38
Na_2O	3.62 ± 0.81	1.75–5.61	2.54 ± 1.28	0.96–3.62	1.73 ± 0.53	2.26 ± 0.95	4.14 ± 0.49	6.04 ± 4.14	1.90
K_2O	1.22 ± 0.77	0.29–4.03	0.50 ± 0.54	0.12–0.88	1.27 ± 0.38	1.80 ± 0.61	1.92 ± 0.15	0.67 ± 0.43	1.95
P_2O_5	0.10 ± 0.05	0.03–0.44	0.15 ± 0.03	0.13–0.19	0.09 ± 0.03	0.06 ± 0.03	0.06 ± 0.00	0.10 ± 0.08	
LOI	3.30 ± 1.73	1.53–9.99	8.07 ± 1.53	5.78–8.90	7.68 ± 2.22	4.25 ± 0.59	2.98 ± 0.33	1.48 ± 0.71	0.002
Total	99.30		100.2		100.1	99.76	99.98	100.15	99.79
Sc	9.6 ± 4.4	3.1–26.6	17.2 ± 4.1	11.9–20.4	15.3 ± 5.3	15.5 ± 2.0	9.76 ± 0.02	17.5 ± 11.6	14.7
V	102 ± 30	50–222	127 ± 22	95–143	120 ± 45	134 ± 13	91 ± 1	110 ± 54	
Cr	60 ± 20	21–130	339 ± 187	110–531	373 ± 615	165 ± 25	127 ± 30	517 ± 352	244
Co	10.9 ± 4.6	3–27	31 ± 13	15–41	19.9 ± 12.7	12.1 ± 5.4	9.66 ± 3.74	30.4 ± 19.4	26.7
Ni	31 ± 13	11–76	194 ± 137	76–386	106 ± 108	48 ± 15	49 ± 24	172 ± 114	157

Table 1. *Continued*. The average and range of compositions of analyzed samples from borehole LB-08A, compared to those of fallout suevites, target rocks, and Ivory Coast tektites.[a]

	Metasediments[b] (n = 75)		Light greenish gray meta-graywacke (n = 4)		Fallout suevite (n = 11)[c]	Meta-graywacke and phyllite (n = 7)[d]	Granite dike (n = 2)[d]	Pepiakese granite (n = 3)[d]	Ivory Coast tektites[d]
	Average	Range	Average	Range	Average	Average	Average	Average	Average
Cu	25.7 ± 16.6	2–83	13 ± 9	6–19	24 ± 21	15.5 ± 7.5	10.7 ± 7.7	24.3 ± 15.1	
Zn	49 ± 18	11–111	76 ± 12	61–88	73 ± 16	104 ± 13	82 ± 5	90 ± 59	23
As	5.03 ± 5.64	0.09–29.3	84.7 ± 67.3	23.1–161	3.1 ± 1.0	7.00 ± 5.91	14.9 ± 12.3	12.7 ± 6.9	0.45
Rb	47.3 ± 28.3	14–143	17 ± 13	5–35	51.4 ± 17.7	65.2 ± 26.2	69.9 ± 18.7	22.4 ± 19.4	66
Sr	424 ± 104	203–638	608 ± 223	328–854	301 ± 56	152 ± 40	342 ± 31	377 ± 44	260
Y	12 ± 3	7–25	12 ± 1	11–13	16 ± 2	19 ± 5	11 ± 1	11 ± 6	
Zr	118 ± 21	56–171	90 ± 14	78–109	122 ± 19	143 ± 12	129 ± 10	82 ± 21	134
Nb	3.6 ± 0.9	3–7	3	3–3	8.0 ± 2.6	5.7 ± 0.8	3.7 ± 0.3	1.8 ± 1.3	
Sb	0.36 ± 0.22	0.03–0.98	1.59 ± 1.90	0.30–4.39	0.33 ± 0.16	0.20 ± 0.06	0.18 ± 0.04	0.42 ± 0.16	0.23
Cs	2.69 ± 1.40	1.00–7.58	1.08 ± 0.62	0.48–1.93	3.71 ± 3.78	3.27 ± 1.48	4.22 ± 1.49	0.87 ± 0.46	3.67
Ba	599 ± 241	244–1320	155 ± 161	46–387	563 ± 83	454 ± 112	605 ± 109	226 ± 117	327
La	19.4 ± 4.3	11.6–33.0	12.7 ± 2.2	10.5–15.9	18.9 ± 5.1	23.4 ± 8.3	18.8 ± 4.0	15.6 ± 8.2	20.70
Ce	39.5 ± 7.8	23.7–64.2	28.8 ± 5.8	23.8–37.2	38.8 ± 8.5	34.8 ± 11.8	39.4 ± 7.3	32.0 ± 14.9	41.90
Nd	17.2 ± 3.3	11.7–25.9	16.3 ± 4.3	12.5–22.5	18.2 ± 4.8	26.5 ± 10.8	19.8 ± 6.4	17.5 ± 9.2	21.80
Sm	3.10 ± 0.63	1.86–4.97	3.28 ± 0.64	2.81–4.17	3.53 ± 0.74	5.06 ± 1.68	3.74 ± 0.25	3.58 ± 1.87	3.95
Eu	0.93 ± 0.18	0.55–1.57	0.95 ± 0.12	0.78–1.06	1.07 ± 0.18	1.29 ± 0.41	1.03 ± 0.14	1.19 ± 0.49	1.20
Gd	2.72 ± 0.87	1.04–5.87	2.66 ± 0.46	2.18–3.08	2.92 ± 0.95	4.80 ± 1.73	3.40 ± 0.00	3.07 ± 1.45	3.34
Tb	0.42 ± 0.13	0.19–0.84	0.47 ± 0.09	0.40–0.60	0.47 ± 0.10	0.73 ± 0.27	0.59 ± 0.02	0.47 ± 0.22	0.56
Tm	0.18 ± 0.04	0.11–0.32	0.17 ± 0.02	0.15–0.20	0.33 ± 0.13	0.35 ± 0.11	0.22 ± 0.03	0.20 ± 0.09	0.30
Yb	1.20 ± 0.28	0.64–2.13	1.13 ± 0.13	0.98–1.30	1.57 ± 0.28	2.14 ± 0.46	1.13 ± 0.05	1.18 ± 0.54	1.79
Lu	0.19 ± 0.05	0.10–0.36	0.17 ± 0.02	0.15–0.21	0.23 ± 0.04	0.29 ± 0.05	0.16 ± 0.01	0.14 ± 0.07	0.24
Hf	3.08 ± 0.68	1.20–5.09	2.34 ± 0.20	2.14–2.60	3.22 ± 0.24	4.04 ± 0.36	3.66 ± 0.12	1.88 ± 0.91	3.38
Ta	0.33 ± 0.14	0.13–0.95	0.25 ± 0.14	0.17–0.46	0.30 ± 0.08	0.42 ± 0.11	0.28 ± 0.09	0.19 ± 0.08	0.34
W	1.97 ± 1.57	0.05–5.45	3.89 ± 0.06	3.84–3.93		0.64 ± 0.16	0.84 ± 0.04	0.54 ± 0.17	0.36
Th	2.99 ± 0.67	1.58–4.42	1.75 ± 0.20	1.54–2.01	2.94 ± 0.61	3.94 ± 0.56	3.10 ± 0.27	2.21 ± 2.09	3.54
U	1.06 ± 0.54	0.26–3.36	2.02 ± 2.22	0.76–5.34	1.05 ± 0.58	1.35 ± 0.15	1.75 ± 0.11	0.74 ± 0.53	0.94
K/U	11,622 ± 8993	2245–49,525	1337 ± 44	1306–1368	10,568	11,389 ± 4357	9245 ± 1314	10,800 ± 7108	17,287
Zr/Hf	38.9 ± 4.0	26.1–47.1	38.1 ± 3.9	32.8–41.9	37.9	35.5 ± 3.7	35.4 ± 3.9	51.9 ± 19.6	39.6
La/Th	6.56 ± 0.90	3.80–9.01	7.21 ± 0.56	6.65–7.86	6.54	6.15 ± 2.49	6.00 ± 0.77	10.9 ± 5.79	5.85
Hf/Ta	10.0 ± 2.66	3.25–16.4	10.5 ± 3.32	5.66–13.1	11.6	10.1 ± 2.48	14.5 ± 4.08	12.7 ± 7.26	9.94
Th/U	3.32 ± 1.41	0.82–10.6	1.53 ± 0.83	0.33–2.23	3.34	2.95 ± 0.51	1.79 ± 0.27	2.67 ± 0.91	3.77
La_N/Yb_N	11.3 ± 2.82	4.82–18.5	7.75 ± 2.06	6.63–10.8	8.19	7.30 ± 1.93	11.2 ± 1.95	13.7 ± 13.2	7.81
Eu/Eu*	0.99 ± 0.11	0.81–1.51	0.99 ± 0.07	0.92–1.08	1.10	0.83 ± 0.14	0.88 ± 0.09	1.16 ± 0.13	1.01
CIA	55	41–73	46	41–49	70	72	63	47	

[a]Major element data in wt%, trace element data in ppm. All Fe as Fe_2O_3. n = number of samples; N = chondrite-normalized (Taylor and McLennan 1985); chemical index of alteration (CIA) = $(Al_2O_3/[Al_2O_3 + CaO + Na_2O + K_2O]) \times 100$ in molecular proportions. All ratios are the average of the ratios calculated for each samples.

[b]Average of 68 meta-graywacke and 8 phyllite-slate samples.

[c]Data from Boamah and Koeberl (2003).

[d]Data from Koeberl et al. (1998).

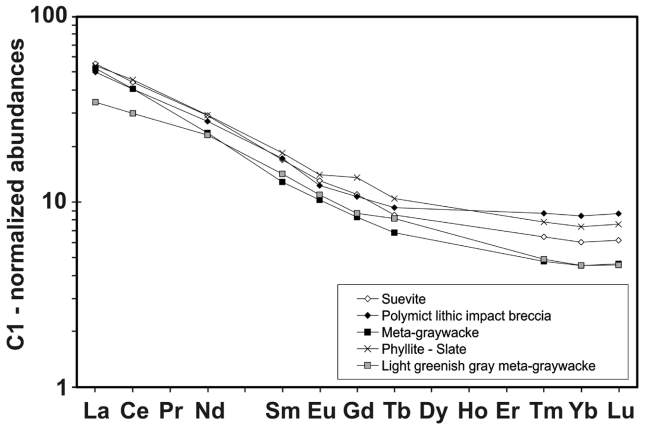

Fig. 3. Chondrite (C1)-normalized rare earth element distribution patterns for the averages of the various lithologies of core LB-08A. The ranges and patterns for the impact breccias and the various target rocks are very similar, indicating that no significant component that is not represented in the basement section contributed to the impact breccia mixtures and also that post-impact alteration was limited and did not lead to any significant REE anomalies. Normalization factors from Taylor and McLennan (1985).

variations, as well as those that are of geochemical importance, are shown in Figs. 1 and 2 and are discussed here. The chondrite-normalized REE distribution patterns of the averages of the different lithologies in core LB-08A are shown in Fig. 3. In addition, we also present Harker diagrams (Fig. 4) showing the variations in major element contents for all the lithologies present in core LB-08A (suevite, polymict lithic impact breccia, meta-graywacke, phyllite-slate, and light greenish gray meta-graywacke), together with the average value for suevite from outside the northern crater rim (after Boamah and Koeberl 2003). Figure 5 contains the binary diagrams of the abundances of trace elements Ba, Cs, and Rb (in ppm) against K_2O contents (in wt%), showing the relation of the contents of these elements to the abundance of potassic phases in samples from core LB-08A. Figure 6 displays the elemental compositions of the average fallback suevite (from core LB-08A) major and trace element contents normalized to the average fallout suevite composition from outside the northern crater rim.

Major Element Contents

The compositions of the five main lithologies (suevite, polymict lithic impact breccia, meta-graywacke, slate-phyllite, and light greenish gray meta-graywacke [LGMG]) all show substantial variations within each lithology, and also have significant differences between them, especially for SiO_2, Al_2O_3, Fe_2O_3, MgO, and CaO contents (Figs. 1 and 2; Table 1). Meta-graywacke samples display the highest SiO_2 content (70.7 wt% on average; std. dev. = 3.18 wt%) of the five lithologies analyzed and can be easily discriminated from phyllite and slate samples, which have an average SiO_2 content of about 57.8 wt%. Phyllite and slate samples have higher Fe_2O_3 and Al_2O_3 contents than meta-graywacke. Compared to all the other lithologies, the LGMG samples have higher CaO and LOI values (Table 1) and also a very high MgO content. Suevite and polymict lithic impact breccia samples have both very similar SiO_2 contents (63.2 and 61.4 wt% on average, respectively).

In the fallback breccia deposit (between 235.6 and 262 m, see Fig. 1), samples display significant differences for the SiO_2 and CaO contents, from 54.80 to 68.43 wt% and from 0.20 to 6.14 wt%, respectively, and substantial variation for the Al_2O_3, Fe_2O_3, and MgO contents. The same is true for the lithologies in the basement section (between 262 to 451 m; see Fig. 2), where the sample compositions also vary within a substantial range, especially for the SiO_2, Al_2O_3, Fe_2O_3, MgO, and CaO contents. LGMG samples have higher MgO and CaO contents compared to the other lithologies (significant peaks in Fig. 2). The other significant peaks observed for both Fe_2O_3 and Al_2O_3 contents in Fig. 2 result from the presence of phyllite and slate samples.

Trace Element Contents

Some significant variation of trace element contents between lithologies and also within lithological types has been observed (Figs. 1 and 2; Table 1). In the following sections, elements are separated according to their geochemical behavior.

Lithophile and Chalcophile Elements

The abundances of the lithophile elements Ba, Rb, and Sr vary by about an order of magnitude between different samples, with Sr showing less variation than Ba and Rb. The different lithologies have variable Ba contents (also variable within lithological types), but the averages for suevite (626 ppm on average), polymict lithic impact breccia (742 ppm on average), and meta-graywacke (537 ppm on average) are fairly similar to each other. The Ba content of the phyllite-slate samples varies by about a factor of two and on average these rocks have a Ba content that is about ten times higher than that of the LGMG samples (1023 versus 155 ppm). The largest variation in Ba content of any of the lithologies is shown by the polymict lithic breccias.

The Rb content is also variable in the different lithologies (Figs. 1 and 2). Suevite and polymict lithic impact breccia samples have similar contents (67 and 86 ppm, respectively), whereas a higher content is observed in phyllite-slate samples (117 ppm on average), compared to a lower one in meta-graywacke and LGMG samples (38 and 17 ppm, respectively). The Sr content is very variable in the different lithologies and also within lithologies, with higher abundances observed in LGMG samples, and lower abundance in polymict lithic impact breccia. The Sr content is higher (on average) in suevite than in polymict lithic impact breccia.

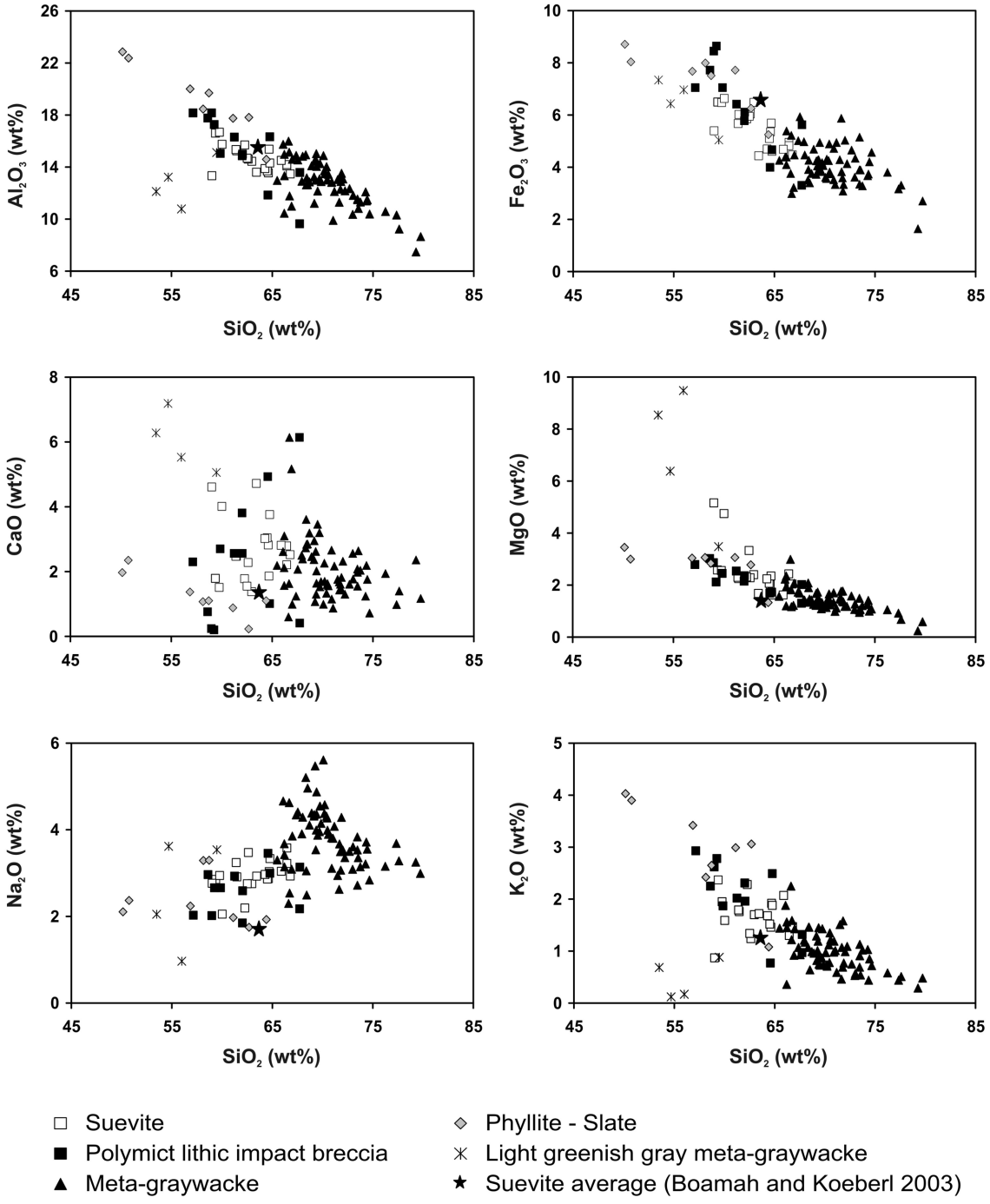

Fig. 4. Harker diagrams for the contents of the major oxides of Al, Fe, Ca, Mg, Na, and K, plotted versus silica content, for suevite, polymict lithic impact breccia, meta-graywacke, phyllite-slate, and light greenish gray meta-graywacke samples from core LB-08A. These data are compared with the average values for suevite from outside the northern crater rim (from Boamah and Koeberl 2003).

The contents of the chalcophile elements Cr, Cu, and Zn show less variation that the lithophile elements discussed above. Chromium contents are very similar for suevite, polymict lithic impact breccia, and phyllite-slate samples (on average), with a wider range for suevite samples. Two suevite samples, KR8-043 and KR8-107 (depths = 296.94 and 422.36 m, respectively) have Cr content about 2.5 times higher than the other suevite samples (significant peaks in Fig. 2). The LGMG samples have a high Cr content (339 ppm on average; maximum Cr content of 531 ppm, significant peaks in Fig. 2) in comparison with the other lithologies. Thus the Cr content is about 6 times higher in LGMG than in other meta-graywacke samples. The Cu contents are in about the same range for suevite and meta-

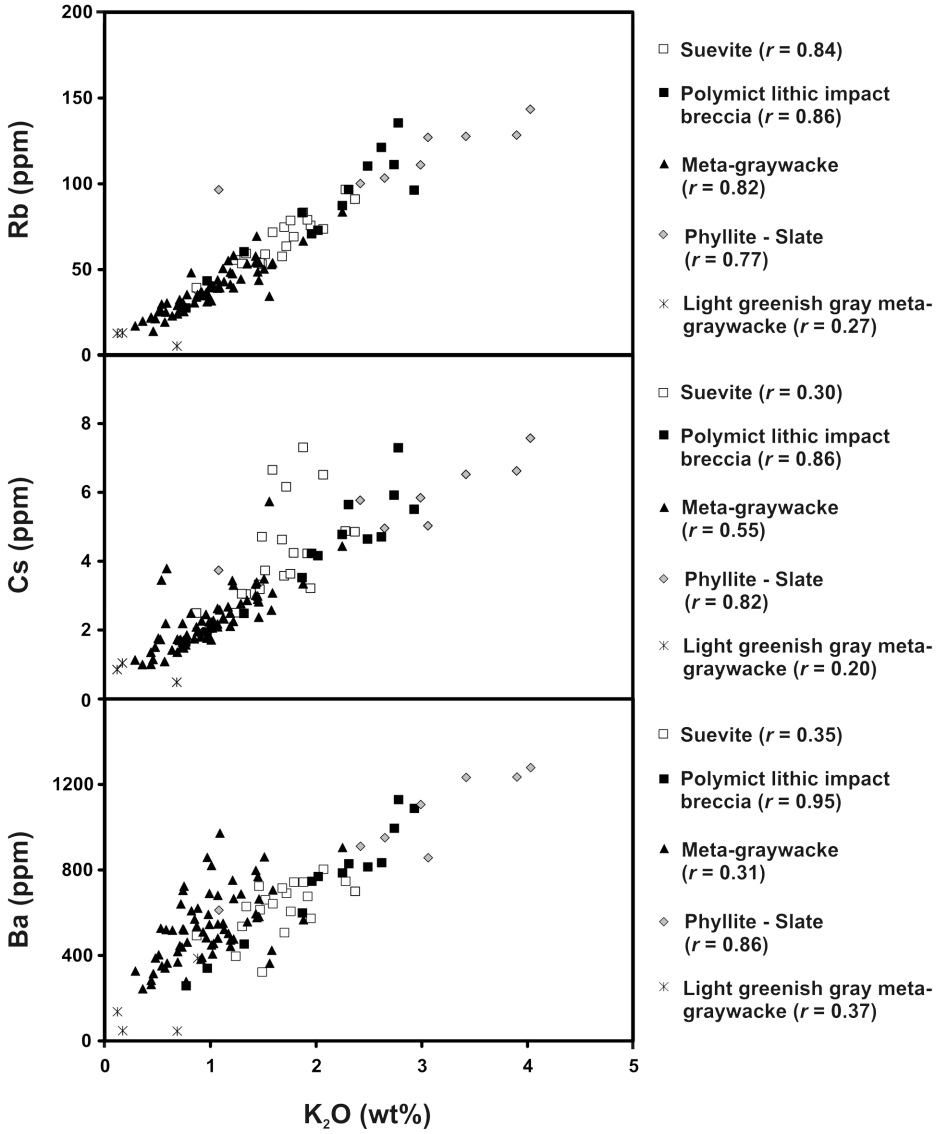

Fig. 5. Binary diagrams comparing the abundances of the trace elements Ba, Cs, and Rb (in ppm) with those of K_2O content (in wt%), showing the degree of correlation between the abundances of these elements for the different lithologies present in core LB-08A (r = correlation coefficient).

graywacke samples (about 25 ppm on average) and higher in both polymict lithic impact breccia and phyllite-slate samples (41 and 44 ppm on average, respectively). The Zn contents in suevite, polymict lithic impact breccia, and LGMG samples are somewhat similar (between 66 to 76 ppm on average), higher in phyllite-slate samples (94 ppm in average) and lower in meta-graywacke samples (43 ppm in average).

Siderophile Elements

The Co and Ni contents are very similar for suevite, polymict lithic impact breccia, and phyllite-slate samples (on average), with higher standard deviations for suevite samples (Table 1). The LGMG samples have higher Co and Ni contents (31 and 194 ppm on average, respectively) than the other lithologies (up to 41 and 386 ppm, respectively, significant peaks like for Cr content in Fig. 2). The Ni content is about 7 times higher in LGMG than in meta-graywacke samples. The Co and Ni contents are two times lower in meta-graywacke samples than in phyllite-slate samples. The two suevite samples (at 296.94 and 422.36 m, respectively) that display higher Cr content than the other suevite samples (discussed earlier) have also Ni content about three times higher than the other suevite samples (significant peaks in Fig. 2). Gold contents are generally very high compared to average crustal abundances (e.g., Taylor and McLennan 1985), and Ir contents are below the detection limit (of about 1 to 2 ppb) for all samples.

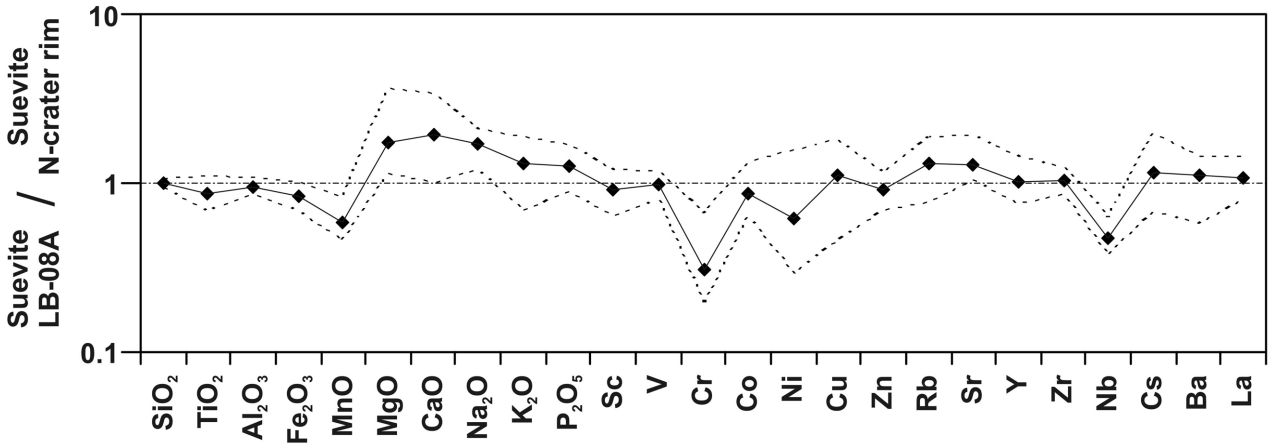

Fig. 6. Major and trace element contents for the average composition of suevites in core LB-08A, normalized to the average composition of suevite from outside the northern crater rim (Boamah and Koeberl 2003). Dashed lines indicate the maximum range of the ratios.

Rare Earth Elements (REE)

As shown in Fig. 3, the chondrite-normalized distribution patterns for the rare earth elements (REE) for all samples from core LB-08A are quite similar to each other and the ranges of contents for all lithologies overlap. All samples are enriched in both light rare earth elements (LREE) and heavy rare earth elements (HREE) relative to chondritic values. Only phyllite and slate samples and some of the meta-graywacke samples display minor, mostly negative Eu anomalies, which are not visible on Fig. 3 due to averaging the 67 meta-graywacke samples (Table 1). No Ce anomaly is evident in the analyzed samples.

Correlation Coefficients and Factor Analysis

To investigate correlations between the abundances of different chemical elements in the various lithologies present in core LB-08A, a correlation matrix, containing correlation coefficients between different pairs of major and trace elements, was calculated (Fig. 7). In addition, the compositions of 100 LB-08A samples, of different lithologies (suevite, polymict lithic impact breccia, and meta-graywacke, respectively) were analyzed by factor analysis using the SPSS program (version 11.0), to detect more complex interactions between the different chemical elements. Factor analysis is one of the best methods to reduce observed associations between numerous variables to a small number of fundamental "factors." These "factors" identify groups of elements that behave in similar ways, and are, in most cases, indicative of specific geochemical processes. The abundance data were recalculated using a logarithmic transformation. For the factor analysis, we used the classical principal factor analysis (PFA) option and the method of factor rotation called "varimax" (orthogonal rotations, i.e., the rotated factors are not correlated). For more information about practical aspects, possibilities, and problems of factor analysis in geochemistry, see, e.g., Reimann et al. (2002). The results of the factor analysis are summarized in Figs. 8 and 9, where the x-axis corresponds to the variance for the whole data set for each factor and the y-axis shows the factor loadings of the different chemical elements considered. These figures display the different factors, which account for about 80 to 90% of the total variance of major and trace elements considered, but also the relative importance (or loading) of each element within each factor. It is clear that, for example, the variance of Fe_2O_3, TiO_2, Zn, and V is quasi-exclusively controlled by factor 1 in the three lithologies (Figs. 8 and 9). Moreover, in the three lithologies, the siderophile elements, such as Ni, Cr, and Co, are totally controlled by factors 1 and 2. Factor 3 in the case of the meta-graywacke samples (Fig. 9) has high loadings for the variables Na_2O and Sr, and is interpreted to represent the variation of feldspar contents. In suevite samples, factor 3 is highly loaded by Ba, K_2O, and Rb, and is interpreted to represent the variations of K-feldspar. Factors 4 and 5 in suevite and meta-graywacke samples, and factors 3 and 4 in polymict lithic impact breccia samples, respectively, have very high loadings for the variables MnO, CaO, and LOI (also P_2O_5 and Sr in suevite and in polymict lithic impact breccia samples, respectively). Mainly because of the high loading of LOI in these factors (Figs. 8 and 9), this parameter has an important role and suggests that these factors are mainly controlled by secondary processes.

Mixing Calculations

In order to model the compositions of suevite and polymict lithic impact breccia lithologies, we performed a series of mixing calculations, using the Harmonic Least-Squares (HMX) mixing calculation program (Stöckelmann and Reimold 1989). The average compositions of the three principal target groups used in the calculations are given in Table 1. For additional information on the refinement control

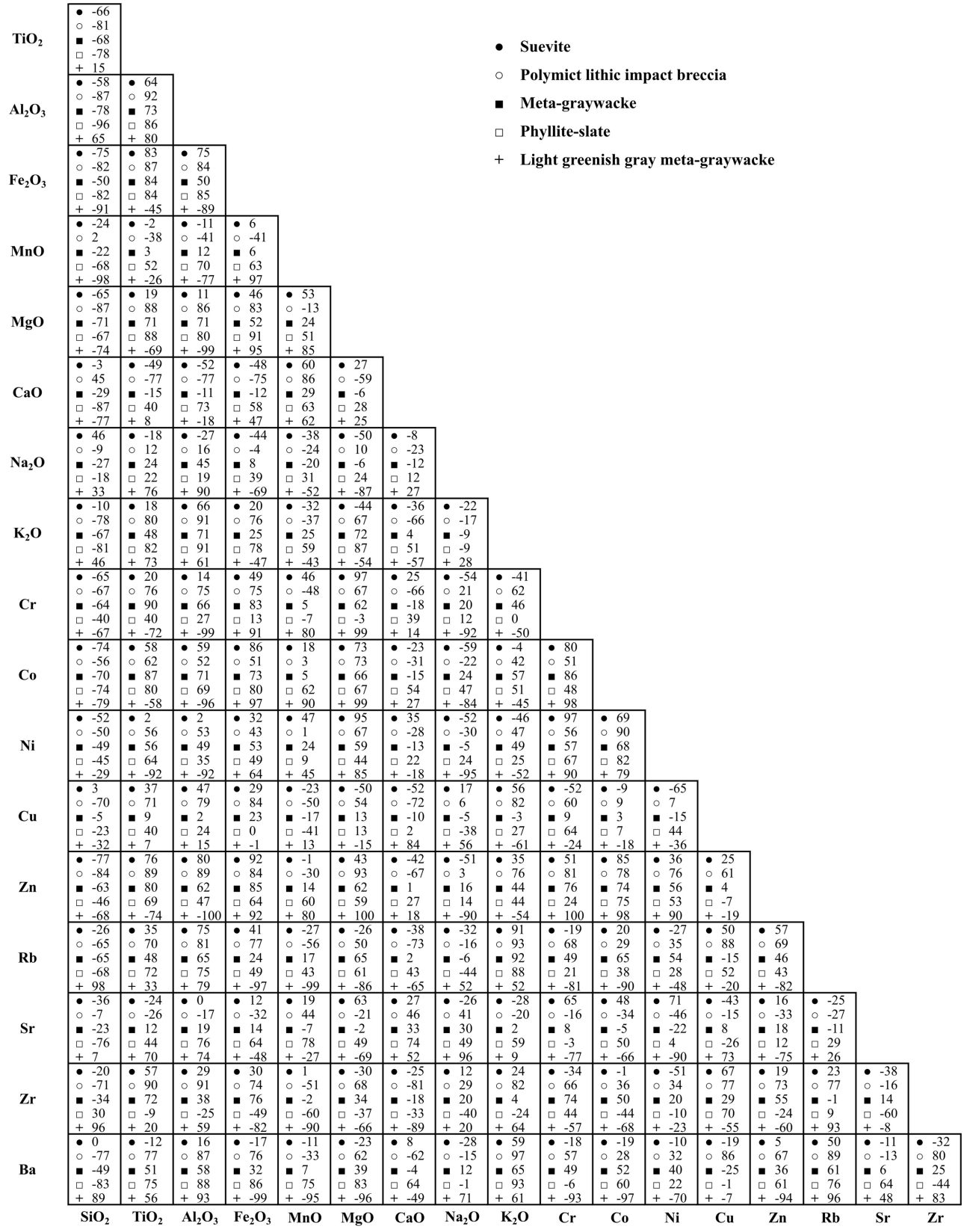

Fig. 7. Correlation coefficient *r* for various element pairs for the five different lithologies of this drill core (all *r* values are multiplied by 100). The same pair of elements can show positive as well as negative correlation, depending on rock types.

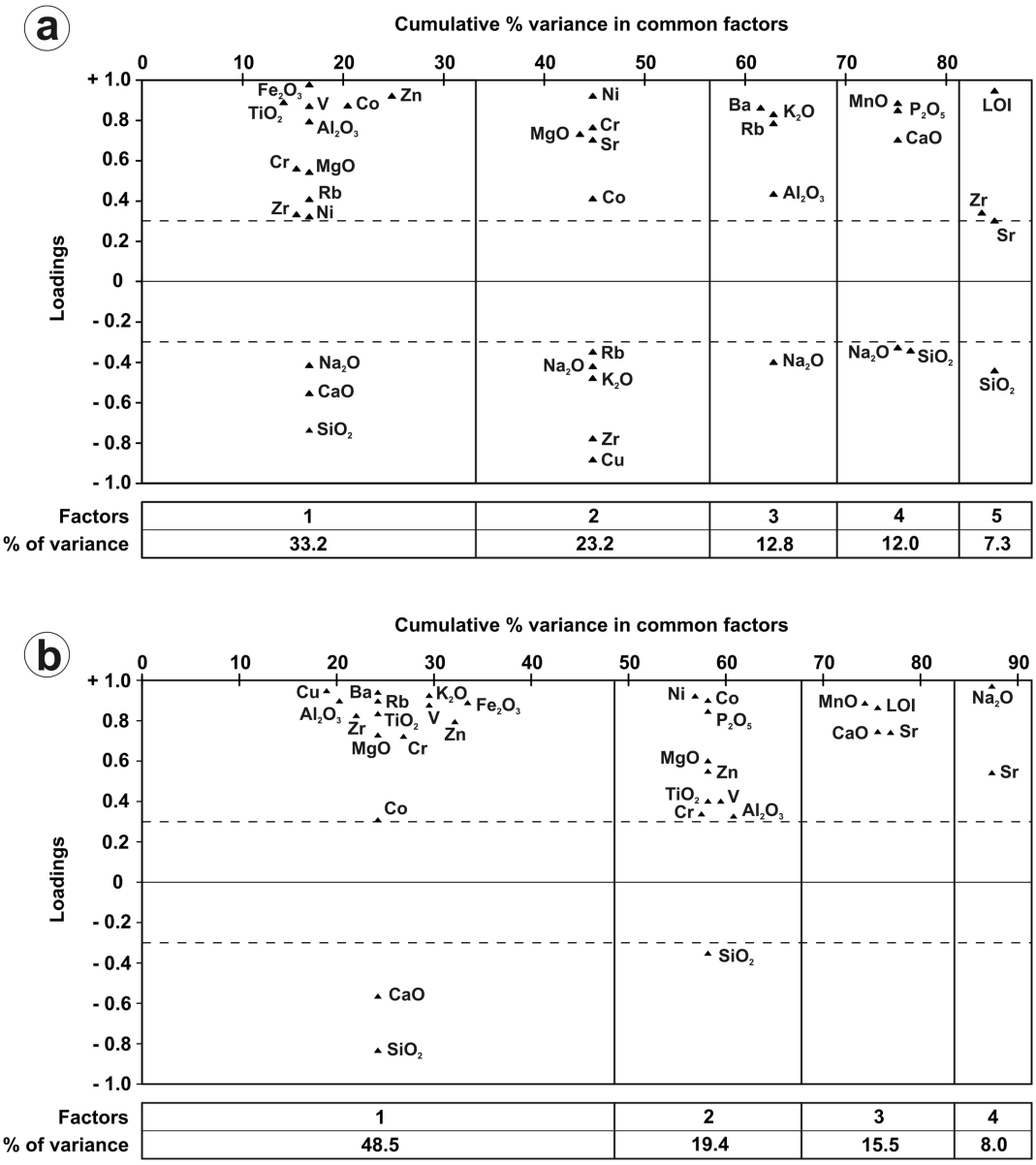

Fig. 8. A graphical representation of the factors extracted from factor analysis (principal factor analysis [PFA], Varimax rotation) for (a) suevite and (b) polymict lithic impact breccia samples. Number of elements = 21; number of samples = 20 for (a) and 13 for (b). The triangles represent the load factor for each element; loadings below 0.3 are not plotted here (they are considered as not significant). The width of the rectangles is proportional to the variance of each factor.

parameters for the purpose of setting different constraints on the mixing calculations, see Stöckelmann and Reimold (1989). Four calculation runs were performed, with major elements only, and others with major elements in combination with some trace elements that are different in abundance from component to component (i.e., the lithologies). Results are summarized in Table 2. Addition of the alkali elements and some trace elements to the calculations did not change the results appreciably (by not more than of a few percent of variation) (Table 2). The mobility of the alkali elements, which could be the result of post-impact alteration, seems to have no effects on the mixing calculations. The discrepancy factors, which indicate the validity of the results (goodness of fit of the mixing calculations), are excellent in all reported calculation runs (Table 2). The observed and calculated mixture compositions for suevite and polymict lithic impact breccia lithologies are compared in Table 3. In both cases, the calculations yield results that are in good agreement with the petrographic observations (Ferrière et al. 2007): the target-rock components of suevite samples are dominated by meta-graywacke and phyllite-slate, with a very small proportion of LGMG. However, it seems that the abundance of the LGMG

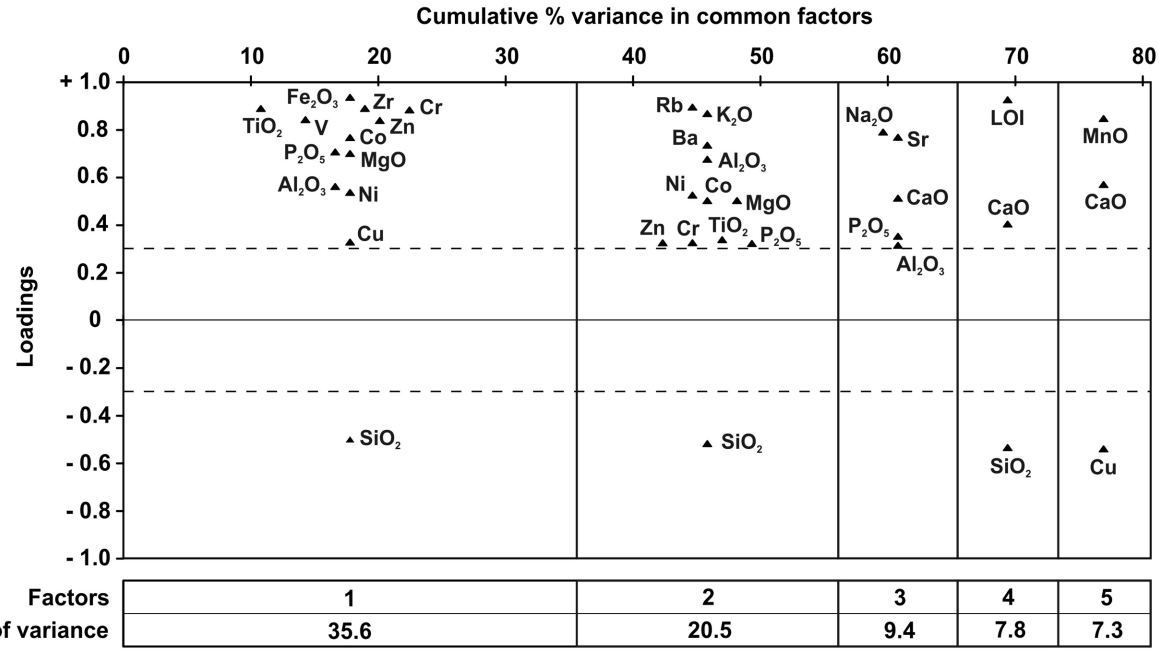

Fig. 9. A graphical representation of the factors extracted from factor analysis (principal factor analysis [PFA], Varimax rotation) for meta-graywacke samples. Number of elements: = 21; number of samples = 67. The triangles represent the load factor for each element; loadings below 0.3 are not plotted here (they are considered as not significant). The width of the rectangles is proportional to the variance of each factor.

Table 2. The results of HMX mixing calculations to reproduce Bosumtwi suevite and polymict lithic impact breccia compositions from contributions from the different lithologies actually identified in the LB-08A drill core.

	Target rock components			
	Meta-graywacke	Phyllite-slate	Light greenish gray meta-graywacke	Discrepancy factor
Suevite [1]	48.9 ± 1.4	34.6 ± 1.4	16.5 ± 1.4	0.33
Suevite [2]	50.9 ± 1.4	31.4 ± 1.6	17.7 ± 1.4	0.21
Suevite [3]	49.4 ± 1.1	34.6 ± 1.2	16.1 ± 1.0	0.28
Suevite [4]	49.2 ± 1.2	35.2 ± 1.3	15.6 ± 1.2	0.32
Polymict lithic breccia [1]	35.7 ± 2.0	60.8 ± 2.3	3.4 ± 1.2	0.44
Polymict lithic breccia [2]	36.1 ± 2.6	61.0 ± 3.1	2.9 ± 1.3	0.38
Polymict lithic breccia [3]	35.3 ± 1.8	60.3 ± 2.1	4.4 ± 0.7	0.42
Polymict lithic breccia [4]	33.5 ± 1.8	63.4 ± 1.9	3.1 ± 0.9	0.45

Run numbers: [1] all major elements, except Mn and P, components total 100%; [2] major elements, except Mn, Na, K, and P, components total 100%; [3] as in run 1 but including Cr and Ni; [4] as in run 1 but including Sc and Th; mixing proportions given in %. Discrepancy factor = goodness of fit (a lower number is best). Harmonic mixing calculations after Stöckelmann and Reimold (1989). Average of target-rock compositions from Table 1.

lithology is overestimated in the calculated suevite mixture composition. The mixing calculations with the polymict lithic breccia composition yielded the highest proportion of the phyllite-slate components (about 60%) in comparison to the ~36% of the meta-graywacke components.

DISCUSSION

In the Harker diagrams (Fig. 4), the data for all lithologies (except the LGMG samples) show a clear inverse correlation between the contents of SiO_2 and the other major oxides: Al_2O_3, Fe_2O_3, MgO, and K_2O, but not for Na_2O. The different lithologies show scattered distributions, which are clearly evident for meta-graywacke and phyllite-slate samples, and with some overlap between suevite and polymict lithic impact breccia samples. This overlap is due to the fact that both suevite and polymict lithic impact breccia are derived from a mixture of similar target rocks (mainly meta-graywacke, phyllite, and slate; Ferrière et al. 2007). No significant correlation between the SiO_2 and CaO contents (Fig. 4) is evident for suevite, polymict lithic impact breccia, and meta-graywacke samples, which could be evidence for overprint from a secondary, post-impact calcium carbonate component. Curiously, the SiO_2 and CaO contents show a normal correlation in phyllite-slate and LGMG samples (Figs. 4 and 7), which is not yet understood. We have also observed a tendency of increasing CaO content in meta-graywacke samples with increasing depth in the lower part of the basement

section (in between 320 and 451 m) (Fig. 2), which might be due to an increase in the abundance of secondary calcite veinlets and aggregates with depth. This tendency has not been yet confirmed by microscopic observations of the distribution of calcite veinlets and aggregates with depth in the meta-graywacke samples from the basement (Ferrière et al. 2007).

The LGMG samples have higher CaO and LOI values than all other lithologies (Table 1; Fig. 4), which could be related to the presence of significant amounts of calcite pods in the LGMG samples (in agreement with observations by Ferrière et al. 2007). The LOI values are about two times higher for LGMG samples than for the other lithologies (8.07 wt% on average), which indicate the presence of a significant amount of volatiles (water, calcium carbonate). High LOI values are consistent with alteration, which agrees with the petrographic determination of significant amounts of chlorite in the LGMG samples (Ferrière et al. 2007).

In comparison with all the lithologies present in core LB-08A, LGMG samples also have very high MgO contents of about 7 wt% (Table 1; Fig. 4), five times higher than the content in the meta-graywacke and about three times higher than in the other lithologies. This high MgO abundance could be related to abundant chlorite (Ferrière et al. 2007) present in the LGMG samples. Interestingly, the MgO content is about two times higher in two suevite samples (KR8-043 and KR8-107; depths = 294.94 and 422.36 m, respectively; Fig. 4) than in other suevite samples. These observations are in agreement with the presence of clasts of the LGMG lithology (that contains abundant chlorite) in the KR8-043 and KR8-107 suevite samples, as shown by Ferrière et al. (2007).

The Na_2O content in meta-graywacke samples (3.77 wt% on average) is slightly higher than the contents in the "meta-graywacke and phyllite lithology" from outside the crater (2.26 wt% on average; Table 1), and the Na_2O abundance varies from 2.30 to 5.61 wt% within the meta-graywacke lithology. These variations of the Na_2O content can be mainly credited to the variable albite abundances in the different meta-graywacke samples (Ferrière et al. 2007).

The Rb content is clearly correlated with K_2O content (Figs. 5 and 7) in all the samples from core LB-08A (except for LGMG samples; correlation coefficient of 0.57), suggesting that this element is mostly incorporated in potassic phases (such as K-feldspar and some phyllosilicate minerals). The Cs and Ba contents do not correlate well with the K_2O contents in suevite, meta-graywacke, and LGMG samples. On the other hand, the Cs and Ba contents show good correlations with the K_2O, Al_2O_3, and Fe_2O_3 content in polymict lithic impact breccia and phyllite-slate samples (Figs. 5 and 7), suggesting that Cs and Ba elements are mainly incorporated in K-feldspar and phyllosilicate minerals (e.g., Shaw 1956).

The Sr contents vary for the different lithologies and within lithological types (Table 1) and are higher in suevite than in polymict lithic impact breccia (387 and 291 ppm on average, respectively). Strontium concentrations are in part controlled by plagioclase abundance (Rollinson 1993; however, no specific difference of plagioclase abundance in polymict impact breccia samples has been noted by Ferrière et al. 2007).

Table 3. A comparison of measured suevite and polymict lithic impact breccia compositions with those obtained from the mixing calculations.

	Suevite		Polymict lithic breccia	
	Calc. (Run 1)	$\Delta_{obs-calc}$	Calc. (Run 1)	$\Delta_{obs-calc}$
SiO_2	63.43	–0.27	61.93	–0.49
TiO_2	0.55	<0.01	0.60	0.03
Al_2O_3	14.78	–0.13	16.41	–0.71
Fe_2O_3	5.58	–0.09	6.21	0.13
MgO	2.74	–0.24	2.40	–0.09
CaO	2.49	0.18	1.74	0.45
Na_2O	3.00	–0.55	2.83	–0.10
K_2O	1.64	0.03	2.13	–0.05

All data in wt%. $\Delta_{obs-calc}$ = observed value (Table 1) minus calculated value.

The REE patterns (Fig. 3) for all lithologies are very similar, and, indeed, the ranges of the REE contents of the various lithologies overlap. This indicates that the breccias do not contain a significant amount of any exotic lithologies that are not represented by the basement lithologies present in core LB-08A. None of the lithologies show any significant negative Eu anomalies (except a very slight negative Eu anomaly for phyllite-slate samples, of about 0.88 on average), which is typical for Archean crustal rocks, according to Taylor and McLennan (1985). The average Eu/Eu^* values for all lithologies are between about 0.90 and 1.00. The Eu anomalies for some of the lithologies vary somewhat (e.g., 0.8 to 1.5 for metasediments in general), but for most samples the deviations from the average values are very small. The chondrite-normalized REE distribution pattern for the average meta-graywacke, as shown in Fig. 3, does not indicate a negative Eu anomaly because the average value is indistinguishable from unity. Variations of the Eu/Eu^* value are commonly associated with varying abundances of feldspar (mainly plagioclase; Nance and Taylor 1977), but might be also result from the presence of some accessory minerals (Taylor and McLennan 1985). Petrographic observations of meta-graywacke samples from core LB-08A (Ferrière et al. 2007) have shown a large variation in the relative abundance of the different minerals (major minerals, but also accessory minerals) that make up meta-graywacke samples, which could explain the observed variation of the Eu/Eu^* values. The highest La and Ce contents in meta-graywacke samples in comparison with LGMG samples (Fig. 3) can be due to the presence of some accessory minerals in meta-graywacke samples (such as allanite) (Ferrière et al. 2007).

The slightly different patterns for heavy rare earth elements (HREE) (Fig. 3) in suevite and polymict lithic

breccia may be due to the mixture of the various target rock types at somewhat different proportions. The La_N/Yb_N values range from 2.64 to 18.5 (with an average La_N/Yb_N value that is two times higher in meta-graywacke samples that in the other lithologies), which can be the result of the original mixing of the different minerals which constitute samples, or the effect of REE fractionation due to alteration processes. The absence of significant Ce anomalies indicates that post-impact aqueous alteration was either not particularly severe, or did not involve large volumes of fluids percolating through the breccia units.

The chemical index of alteration (CIA) (Table 1) is, in average, very similar for suevite, polymict impact breccia, and meta-graywacke (CIA = 56, 60, and 54, respectively), somewhat higher for phyllite-slate samples (CIA = 67) and lower for LGMG samples (CIA = 46). Suevite, polymict lithic impact breccia, and meta-graywacke samples display a large variation of the CIA values, which suggest some variation in the degree of alteration for the various samples, and possibly also because of the presence of heavy minerals, such as zircon.

As noted above, the abundances of the chalcophile and siderophile elements chromium, vanadium, nickel, and cobalt vary between the different lithologies, but also within lithological types (Table 1). Cobalt is well correlated with the Fe_2O_3 content in most lithologies (not correlated well in polymict lithic impact breccia samples) (Fig. 7), suggesting that this element is mainly incorporated in sulfide minerals (such as pyrite), biotite, and chlorite minerals. Chromium and nickel contents are also rather well correlated with the MgO abundance (correlation coefficients between 0.85 and 0.99) (Fig. 7) in both suevite and LGMG samples, which can again be explained by these elements being contained mainly in phyllosilicate minerals, as well as in sulfide minerals such as pyrite (Ferrière et al. 2007) or pyrrhotite (Kontny and Just 2006). The large standard deviations on the average Cr and Ni contents for suevite samples (std. dev. = 57 and 31 ppm, respectively) are mainly due to the presence of two suevite samples, KR8-043 and KR8-107 (depths = 296.94 and 422.36 m, respectively), which have Cr contents more than twice the average suevite value (249 and 238 ppm, respectively), compared to about 115 ppm on average (significant peaks in Fig. 2) and Ni contents about three times that of the average suevite (165 and 156 ppm, respectively, compared to 50 ppm on average). The presence of LGMG clasts in these two suevite samples (Ferrière et al. 2007) can explain these abnormally higher Cr and Ni contents in comparison to the average of Cr and Ni abundances for suevite (significant peaks in Fig. 2). This observation indicates that local rock fragments (only transported a few centimeters; angular clasts) are incorporated into the suevite dikelets (see also Ferrière et al. 2007). These authors also noticed that these suevite dikelets are more severely altered (abundant phyllosilicate minerals) than the surrounding metasediments.

The siderophile element data show similar abundances for polymict impact breccia and for phyllite-slate samples (Table 1), as well as for the meta-graywacke samples. The observation that the various impact breccias do not show any anomalous enrichment in the siderophile element contents compared to the target rocks, indicates that there is no immediate evidence for the presence of a meteoritic component. This is in agreement with previous work by Dai et al. (2005), who studied platinum group elements in impactites from outside the crater and have not detected the presence of a meteoritic component in Bosumtwi impactites. These results by Dai et al. (2005) also confirm the high indigenous abundances of the siderophile elements, and these authors concluded that elemental data alone cannot be used to verify the presence of a meteoritic component in Bosumtwi crater rocks. On the other hand, Koeberl and Shirey (1993) found an extraterrestrial component in Ivory Coast tektites and Bosumtwi impact glass (isolated from suevites), using the Os isotopic method method; this was confirmed by Cr isotopic studies by Koeberl et al. (Forthcoming). Numerical modeling of the formation of Bosumtwi (Artemieva et al. 2004) predicted that the extraterrestrial material should be heterogeneously distributed within the crater with 0.1% or less of a projectile component in samples from inside the crater. Artemieva et al. (2004) also predicted that there is a higher probability of finding a projectile component in downrange distal ejecta (to the west-southwest of the crater center, according to the position of the Ivory Coast tektites strewn field) and also a substantial amount in proximal ejecta near the crater rim in a downrange direction (Artemieva et al. 2004). These predictions are partially in accordance with our observations, as well as those of Dai et al. (2005) and Koeberl and Shirey (1993). However, the absence of any significant melt-rich-suevite layer in the central part of the crater (Ferrière et al. 2007), which was assumed to be present based on geophysical as well as numerical modeling (Jones et al. 1981; Plado et al. 2000; Artemieva et al. 2004), is noticeable.

Comparison with Chemical Data for Fallout Impact Breccia

For comparison of chemical data for suevite samples from core LB-08A (fallback breccia) and chemical data for suevite from outside the northern crater rim (fallout breccia; cf. Boamah and Koeberl 2003) we use, in addition to the Harker diagrams (Fig. 4), a diagram showing the contents in average suevite (from core LB-08A) normalized to contents in suevite from outside the northern crater rim (Fig. 6). In both Boamah and Koeberl (2003) and this study, the concentrations were determined by the same methods.

Fallback suevites from LB-08A core and fallout suevite have identical SiO_2 contents (63.2 and 63.6 wt% on average, respectively). Regarding the other major elements, the TiO_2, Al_2O_3, and Fe_2O_3 contents are very similar in both suevite

populations (Fe_2O_3 contents are slightly lower in fallback suevite); the MnO, MgO, CaO, and Na_2O contents are very different in both suevite types (this regards the average compositions as well as the maxima and minima) (Fig. 6). Specifically, the MnO content is lower in fallback suevite than in fallout suevite samples, whereas the MgO, CaO, and Na_2O contents are higher in fallback suevite than in fallout suevite samples. The K_2O and P_2O_5 contents are slightly higher in fallback suevite from core LB-08A, but still within the range of contents in fallout suevite samples. These differences in some major element abundances can be the result of a difference in clast populations in both suevite populations (calcite clasts are present in fallback breccia and not in fallout suevite, and granite clasts are present in fallout suevite and not in fallback breccia; Ferrière et al. 2007) or might suggest a higher post-impact aqueous alteration in suevite samples from core LB-08A than in fallout suevites samples.

The trace element contents in both suevite populations are very similar (Fig. 6), with the exception of the abundances of Cr, Nb, and Ni. The Ni content is lower in fallback suevite than in fallout suevite samples, but the ranges overlap (31 to 165 ppm versus 52 to 423 ppm, respectively). Chromium and Nb are relatively depleted in fallback suevite from core LB-08A, by factors of 3 and 2, respectively, compared to fallout suevite. This enrichment of Cr and Ni in fallout suevite (in comparison with fallback suevite) could be due to a difference in clast populations that constitute both suevite samples. For example, granite clasts have been observed in suevite from outside the northern crater rim (up to 3 vol% of granitic clasts) (Boamah and Koeberl 2003, 2006) but not in suevite from core LB-08A (Ferrière et al. 2007), and only rare granite clasts, observed in suevite from core LB-07A (Coney et al. 2007). However, the contents of Cr and Ni in a few granite dike samples analyzed by Koeberl et al. (1998) are too low and cannot explain the enrichment in these elements in fallout suevite. On the other hand, the Pepiakese granite (Table 1) (Koeberl et al. 1998) shows high Cr and Ni contents (517 and 172 ppm on average, respectively), but cannot explain the enrichment observed for these elements in fallout suevite (at least about 40 mass% of Pepiakese granite mix into the fallout suevite is necessary to explain these values, which is not realistic). The MnO content in Pepiakese granite (0.067 wt% on average [Koeberl et al. 1998]) seems also to be too low to explain the enrichment in MnO in fallout suevite (in comparison with fallback suevite). Thus, for the time being we cannot readily explain the difference in Cr and Ni contents between the fallback and fallout suevites.

In terms of implications for the understanding of excavation and depositional processes, the differences in the chemical compositions between the fallback and fallout suevites do not allow a clear separation between what is the result of the impact itself and what was induced by secondary alteration processes.

Comparison with Chemical Data for Target Rocks Outside the Crater Rim

The target rocks at Bosumtwi include a variety of lithologies, mainly meta-graywacke, phyllite, shale, granite dikes, and Pepiakese granite (chemical data for each target rocks lithologies are reported in Table 1 for comparison; data from Koeberl et al. 1998). In the basement section of core LB-08A, granite dikes and Pepiakese granite of the target rock types (found in the wider crater region) are definitely absent, and shale occurs only in the form of clasts in the top of the fallback breccia deposit. Earlier papers have not distinguished, as in our study, between meta-graywacke and phyllite samples, but presented an average composition of both lithologies ("graywacke-phyllite" lithology; Table 1; data in Koeberl et al. 1998). To allow a comparison between metasediments in core LB-08A and metasediments from outside the crater rim, we have calculated an average composition for all the metasediments present in core LB-08A (Table 1).

The major element composition of the average graywacke-phyllite from outside the crater rim is within the range of composition of the metasediments from core LB-08A. However, on average, the CaO and Na_2O contents are significantly higher in metasediment from core LB-08A, whereas the Al_2O_3, Fe_2O_3, and MgO contents are slightly higher in graywacke-phyllite from outside the crater rim (Table 1). The higher Al_2O_3, Fe_2O_3, and MgO contents in graywacke-phyllite from outside the crater rim can easily be explained by the fact that a larger number of phyllite samples (having a high content of phyllosilicate minerals) was used in the calculation of the average metasediment from outside the crater rim than in the respective calculation for core LB-08A. The slightly lower SiO_2 content observed for the average of data for metasediment samples from outside the crater rim confirms this higher proportion of phyllite. However, the difference in meta-graywacke and phyllite proportions for the average calculation cannot explain the higher CaO and Na_2O contents observed in metasediment from core LB-08A. These differences in the CaO and Na_2O contents could be the signature of secondary alteration, which affected the basement after the impact event, or simply a result of the original mixing of the different metasediments.

Chromium contents in metasediment from outside the crater rim are more than 1.5 times higher than in the phyllite-slate sample average from core LB-08A and also higher than the maximum Cr content observed in phyllite-slate from core LB-08A (Table 1). Chromium contents are correlated with TiO_2 and Fe_2O_3 abundances in meta-graywacke samples from core LB-08A (Fig. 7), which argues in favor of the localization of the Cr element in magnetite.

Regarding the other trace elements, metasediment compositions from core LB-08A are similar to the composition of the metasediment from outside the crater rim,

except for Sr, which has an abundance three to four times higher in metasediment from core LB-08A. This difference in Sr content might be due to a higher aqueous alteration of samples from core LB-08A than of target rock samples, or to a difference of plagioclase abundance (Rollinson 1993).

During this study we have observed a slight Eu anomaly in phyllite-slate and also in meta-graywacke samples (the Eu anomaly present in several meta-graywacke samples isn't visible on Fig. 3, due to the averaging), similar to the Eu anomaly that was observed in "shale" and "graywacke-phyllite" lithologies (Boamah and Koeberl 2003; Dai et al. 2005) from the target rocks.

SUMMARY AND CONCLUSIONS

A large number of samples of polymict impact breccia (33 samples) and metasediment (79 samples) from the central uplift of the Bosumtwi crater were analyzed for their major and trace element composition.

Five different lithologies have been distinguished on the basis of petrographic observations (Ferrière et al. 2007), comprising polymict lithic impact breccia, suevite, meta-graywacke, slate-phyllite, and light greenish gray meta-graywacke; all these lithologies show significant differences between them, especially for SiO_2, Al_2O_3, Fe_2O_3, MgO, and CaO contents and also substantial variations within lithological types. Suevite and polymict lithic impact breccia samples have both very similar SiO_2 contents (63.2 and 61.4 wt% on average, respectively), in between the SiO_2 content of meta-graywacke samples (70.7 wt% on average) and the SiO_2 content of phyllite-slate samples (57.8 wt% on average). A clear inverse correlation between the contents of SiO_2 and the other major oxides: Al_2O_3, Fe_2O_3, MgO, and K_2O (except for Na_2O) is observed for all lithologies (except for the LGMG samples). The distributions scatter due to the fact that both types of polymict impact breccia are derived from a mixture of target rocks (mainly meta-graywacke and phyllite-slate). No correlation of the SiO_2 and CaO contents for suevite, polymict lithic impact breccia, and meta-graywacke samples have been observed, which might suggest a contribution of a post-impact calcium carbonate component. The CaO content in meta-graywacke samples, which show a tendency of increasing with depth in the lower part of the basement section, can be the result of an increase in the abundance of secondary calcite veinlets and aggregates with depth.

Significant variation of trace element contents between lithologies and also within lithological types has been observed, mainly for Rb, Cs, Ba, and Sr contents. The Cr, Co, and Ni contents are very similar for suevite, polymict lithic impact breccia, and phyllite-slate samples (about 105, 20, and 60 ppm on average, respectively), two times lower in meta-graywacke samples (54, 10, and 27 ppm on average, respectively) and clearly higher in LGMG samples (339, 31, and 194 ppm on average, respectively). Those abundances in Cr, Co, and Ni contents are mainly the result of the localization of these elements in sulfide minerals (such as pyrite and pyrrhotite grains), as well as in phyllosilicate minerals.

The REE patterns, somewhat similar for all samples from core LB-08A, show enrichment in both LREE and HREE relative to chondritic values. The slightly different patterns observed for HREE in suevite and polymict lithic breccia could result from the mixture of the various target rock types at somewhat different proportions. Only the phyllite and slate samples and some meta-graywacke samples display a slight Eu anomaly.

This study also shows the possibility to clearly distinguish the different metasediment lithologies, on the basis of their compositions, using the major element abundances and Sc, Cr, Co, Ni, and Zn contents, which are noticeably distinct for these lithologies.

Our main conclusions are:

1. Most of the variations of the major and trace element abundances within each lithology results from variations in the proportions of the mineral constituents of those rocks. However, aqueous alteration processes have definitely affected the different rocks from the core LB-08A, which is shown by the CIA values (from 41 to 73) and by the presence of secondary calcium carbonates; this is in agreement with petrographic observations.
2. The chemical compositions of both the suevite and the polymict lithic breccia from core LB-08A can be closely approximated using the HMX mixing calculation program. A mixture of about 50 wt% meta-graywacke, 34 wt% phyllite-slate, and 16 wt% of LGMG for the suevite composition, and a higher proportion of phyllite-slate (~60%) with ~36% of meta-graywacke for the polymict lithic breccia, have been calculated, and those results are in good agreement with the petrographic observations.
3. Fallback suevite (suevite from core LB-08A) and fallout suevite samples display some differences in major element abundances, mainly in the MgO, CaO, and Na_2O contents that could be related to the higher degree of alteration of samples from fallback suevite than fallout suevite samples. Some differences in the clast populations of the two suevite facies (no granite clasts have been observed in samples from core LB-08A and no calcite clasts in fallout suevite), can also induce some variations of major and trace element abundances.
4. No significant difference exists between the chondrite-normalized REE patterns for the different lithologies studied in core LB-08A and the fallout suevite and target rocks from outside the crater rim, suggesting that the major constituents of both suevite populations represent the same target rock types.
5. No evidence for a meteoritic component has been detected during this study (similar siderophile element contents observed for polymict impact breccia and for

phyllite-slate samples), which is in agreement with previous works. Complementary analyses, such as platinum group element analyses and related isotopic studies, are necessary to investigate any possible extraterrestrial component in fallback breccia.

Acknowledgments–Drilling at Bosumtwi was supported by the International Continental Scientific Drilling Program (ICDP), the U.S. NSF-Earth System History Program under grant no. ATM-0402010, Austrian FWF (project P17194-N10), the Austrian Academy of Sciences, and by the Canadian NSERC. We are grateful to DOSECC, Inc., for the drilling operations. This work was supported by the Austrian FWF (P17194-N10, to C. K.). We appreciate the help of H. Böck, M. Villa, M. Bichler, and G. Steinhauser (Atominstitut Vienna) with the irradiations. We are grateful to D. Kring and G. Osinski for constructive reviews.

Editorial Handling—Dr. Bernd Milkereit

REFERENCES

Artemieva N. A., Karp T., and Milkereit B. 2004. Investigating the Lake Bosumtwi impact structure: Insight from numerical modeling. *Geochemistry Geophysics Geosystems* 5, doi:10.1029/2004GC000733.

Boamah D. and Koeberl C. 2002. Geochemistry of soils from the Bosumtwi impact structure, Ghana, and relationship to radiometric airborne geophysical data. In *Meteorite impacts in Precambrian shields*, edited by Plado J. and Pesonen L. Impact Studies, vol. 2. Heidelberg: Springer. pp. 211–255.

Boamah D. and Koeberl C. 2003. Geology and geochemistry of shallow drill cores from the Bosumtwi impact structure, Ghana. *Meteoritics & Planetary Science* 38:1137–1159.

Boamah D. and Koeberl C. 2006. Petrographic studies of "fallout" suevite from outside the Bosumtwi impact structure, Ghana. *Meteoritics & Planetary Science* 41:1761–1774.

Brodie K., Fettes D., Harte B., and Schmid R. 2004. Structural terms including fault rock terms. http://www.bgs.ac.uk/scmr/docs/paper_3/scmr_struc2.pdf. Accessed 16 March 2007.

Coney L., Gibson R. L., Reimold W. U., and Koeberl C. 2007. Lithostratigraphic and petrographic analysis of ICDP drill core LB-07A, Bosumtwi impact structure, Ghana. *Meteoritics & Planetary Science* 42. This issue.

Dai X., Boamah D., Koeberl C., Reimold W. U., Irvine G., and McDonald I. 2005. Bosumtwi impact structure, Ghana: Geochemistry of impactites and target rocks, and search for a meteoritic component. *Meteoritics & Planetary Science* 40: 1493–1511.

Ferrière L., Koeberl C., and Reimold W. U. 2007. Drill core LB-08A, Bosumtwi impact structure, Ghana: Petrographic and shock metamorphic studies of material from the central uplift. *Meteoritics & Planetary Science* 42. This issue.

Gentner W., Kleinmann B., and Wagner G. A. 1967. New K-Ar and fission track ages of impact glasses and tektites. *Earth and Planetary Science Letters* 2:83–86.

Gentner W., Storzer D., and Wagner G. A. 1969. New fission track ages of tektites and related glasses. *Geochimica et Cosmochimica Acta* 33:1075–1081.

Govindaraju K. 1994. 1994 compilation of working values and sample description for 383 geostandards. *Geostandards Newsletter* 18:1–158.

Jackson J. A. 1997. *Glossary of geology,* 4th edition. Alexandria, Virginia: American Geological Institute. 769 p.

Jarosewich E., Clarke R. S. J., and Barrows J. N. 1987. The Allende meteorite reference sample. *Smithsonian Contributions to Earth Sciences* 27:1–49.

Jones W. B. 1985. Chemical analyses of Bosumtwi crater target rocks compared with the Ivory Coast tektites. *Geochimica et Cosmochimica Acta* 48:2569–2576.

Jones W. B., Bacon M., and Hastings D. A. 1981. The Lake Bosumtwi impact crater, Ghana. *Geological Society of America Bulletin* 92:342–349.

Junner N. R. 1937. The geology of the Bosumtwi caldera and surrounding country. *Gold Coast Geological Survey Bulletin* 8: 1–38.

Koeberl C. 1993. Instrumental neutron activation analysis of geochemical and cosmochemical samples: A fast and proven method for small samples analysis. *Journal of Radioanalytical and Nuclear Chemistry* 168:47–60.

Koeberl C. and Reimold W. U. 2005. Bosumtwi impact crater, Ghana (West Africa): An updated and revised geological map, with explanations. *Jahrbuch der Geologischen Bundesanstalt, Wien* (*Yearbook of the Austrian Geological Survey*) 145:31–70 (+1 map, 1:50,000).

Koeberl C. and Shirey S. B. 1993. Detection of a meteoritic component in Ivory Coast tektites with rhenium-osmium isotopes. *Science* 261:595–598.

Koeberl C., Bottomley R. J., Glass B. P., and Storzer D. 1997. Geochemistry and age of Ivory Coast tektites and microtektites. *Geochimica et Cosmochimica Acta* 61:1745–1772.

Koeberl C., Reimold W. U., Blum J. D., and Chamberlain C. P. 1998. Petrology and geochemistry of target rocks from the Bosumtwi impact structure, Ghana, and comparison with Ivory Coast tektites. *Geochimica et Cosmochimica Acta* 62:2179–2196.

Koeberl C., Milkereit B., Overpeck J. T., Scholz C. A., Amoako P. Y. O., Boamah D., Danuor S., Karp T., Kueck J., Hecky R. E., King J. W., and Peck J. A. 2007. An international and multidisciplinary drilling project into a young complex impact structure: The 2004 ICDP Bosumtwi Crater Drilling Project—An overview. *Meteoritics & Planetary Science* 42. This issue.

Koeberl C., Shukolyukov A., and Lugmair G. W. Forthcoming. Chromium isotopic studies of terrestrial impact craters: Identification of meteoritic components at Bosumtwi, Clearwater East, Lappajärvi, and Rochechouart. *Earth and Planetary Science Letters.*

Kolbe P., Pinson W. H., Saul J. M., and Miller E. W. 1967. Rb-Sr study on country rocks of the Bosumtwi crater, Ghana. *Geochimica et Cosmochimica Acta* 31:869–875.

Kontny A. and Just J. 2006. Magnetic mineralogy and rock magnetic properties of impact breccias and crystalline basement rocks from the BCDP-drillings 7A and 8A (abstract #1343). 37th Lunar and Planetary Science Conference. CD-ROM.

Leube A., Hirdes W., Mauer R., and Kesse G. O. 1990. The Early Proterozoic Birimian Supergroup of Ghana and some aspects of its associated gold mineralization. *Precambrian Research* 46: 139–165.

Moon P. A. and Mason D. 1967. The geology of ¼° field sheets 129 and 131, Bompata S. W. and N. W. *Ghana Geological Survey Bulletin* 31:1–51.

Nance W. B. and Taylor S. R. 1977. Rare earth element patterns and

crustal evolution—II. Archean sedimentary rocks from Kalgoorlie, Australia. *Geochimica et Cosmochimica Acta* 41: 225–231.

Plado J., Pesonen L. J., Koeberl C., and Elo S. 2000. The Bosumtwi meteorite impact structure, Ghana: A magnetic model. *Meteoritics & Planetary Science* 35:723–732.

Reimold W. U., Koeberl C., and Bishop J. 1994. Roter Kamm impact crater, Namibia: Geochemistry of basement rocks and breccias. *Geochimica et Cosmochimica Acta* 58:2689–2710.

Reimold W. U., Brandt D., and Koeberl C. 1998. Detailed structural analysis of the rim of a large, complex impact crater: Bosumtwi crater, Ghana. *Geology* 26:543–546.

Reimann C., Filzmoser P., and Garrett R. G. 2002. Factor analysis applied to regional geochemical data: Problems and possibilities. *Applied Geochemistry* 17:185–206.

Rollinson H. R. 1993. *Using geochemical data: Evaluation, presentation, interpretation*. Harlow, United Kingdom: Longman. 352 p.

Schnetzler C. C., Pinson W. H., and Hurley P. M. 1966. Rubidium-strontium age of the Bosumtwi crater area, Ghana, compared with the age of the Ivory Coast tektites. *Science* 151:817–819.

Schnetzler C. C., Philpotts J. A., and Thomas H. H. 1967. Rare earth and barium abundances in Ivory Coast tektites and rocks from the Bosumtwi crater area, Ghana. *Geochimica et Cosmochimica Acta* 31:1987–1993.

Scholz C. A., Karp T., Brooks K. M., Milkereit B., Amoako P. Y. O., and Arko J. A. 2002. Pronounced central uplift identified in the Bosumtwi impact structure, Ghana, using multichannel seismic reflection data. *Geology* 30:939–942.

Shaw D. M. 1956. Geochemistry of politic rocks. Part II: Major elements and general geochemistry. *GSA Bulletin* 67:919–934.

Son T. H. and Koeberl C. 2005. Chemical variation within fragments of Australasian tektites. *Meteoritics & Planetary Science* 40: 805–815.

Stöckelmann D. and Reimold W. U. 1989. The HMX mixing calculation program. *Mathematical Geology* 21:853–860.

Taylor S. R. and McLennan S. M. 1985. *The continental crust: Its composition and evolution.* Oxford: Blackwell Scientific Publications. 312 p.

Woodfield P. D. 1966. The geology of the ¼° field sheet 91, Fumso N. W. *Ghana Geological Survey Bulletin* 30:1–66.

Wright J. B., Hastings D. A., Jones W. B., and Williams H. R. 1985. *Geology and mineral resources of West Africa.* London: Allen & Unwin. 187 p.